AN ABSTRACT OF THE THESIS OF

Douglas Albert Coe for the degree Doctor of Philosophy
(Name of Student) (Degree)

Chemistry presented on 6-7-74
(Major Department) (Date)

Title: Infrared and Raman Vibrational Studies of Aluminum Tristetrahydroborate and Cyclopentadienylberyllium Tetrahydroborate

Redacted for privacy

Abstract approved: _____
Dr. J. W. Nibler

Volatile metal tetrahydroborates exhibit both double [$Al(BH_4)_3$, $(C_5H_5)_2Zr(BH_4)_2$] and triple [$Be(BH_4)_2$, $Zr(BH_4)_4$, $Hf(BH_4)_4$] hydrogen bridge structures. In addition, studies indicate that certain gaseous "covalent" compounds [$Be(BH_4)_2$, CH_3ZnBH_4] undergo structural changes upon solidification to yield polymeric chains formed of ionic BH_4^- units. In this work some of these interesting structural possibilities are examined for the $Al(BH_4)_3$ and $C_5H_5BeBH_4$ metal tetrahydroborate systems.

Although several earlier studies have shown $Al(BH_4)_3$ and $Al(BD_4)_3$ to be doubly hydrogen bridged, the point symmetry (D_3 or D_{3h})

and therefore the vibrational assignments are still in question. In an effort to further characterize the vibrational spectra and therefore the structure and bonding in $Al(BH_4)_3$ and $Al(BD_4)_3$, the infrared spectra of gaseous, solid, and matrix isolated and the Raman spectra of liquid and solid $Al(BH_4)_3$ and $Al(BD_4)_3$ are presented. The spectra show $Al(BH_4)_3$ and $Al(BD_4)_3$ to be covalent in the phases studied and a complete assignment of the fundamental vibrations is made, consistent with D_{3h} point symmetry. A number of modifications are made of a previous partial fundamental assignment and the results are seen to be in satisfactory agreement with the product rule. Correlated NMR - Raman spectra over the temperature range -60 to + 80°C suggest that an anomalous temperature dependence reported in the literature for the NMR spectra of $Al(BH_4)_3$ and $Al(BD_4)_3$ may be due to traces of decomposition products.

Infrared and Raman spectra of solid C_5H_5BeCl, $C_5H_5BeBH_4$, and $C_5H_5BeBD_5$ are also presented, along with Raman spectra of the liquid phase, and a complete vibrational assignment is made based on C_{5v} local symmetry for the C_5H_5 ring and C_{2v} local symmetry for the metal tetrahydroborate group. The assignments, which are found to be in satisfactory agreement with the product rule, are consistent with the bonding of the beryllium and boron via two hydrogen bridges. From the results it may also be concluded that the plane of the bridging hydrogens is coincident with the C_s symmetry plane.

Infrared and Raman Vibrational Studies of Aluminum Tristetrahydroborate and Cyclopentadienylberyllium Tetrahydroborate

by

Douglas Albert Coe

A THESIS

submitted to

Oregon State University

in partial fulfillment of
the requirements for the
degree of

Doctor of Philosophy

June 1975

APPROVED:

Redacted for privacy

Associate Professor of Chemistry
in charge of major

Redacted for privacy

Chairman of Department of Chemistry

Redacted for privacy

Dean of Graduate School

Date thesis presented June 7, 1974

Typed by Anna E. Coe for Douglas Albert Coe

ACKNOWLEDGMENT

I would like to thank Dr. J. W. Nibler for his inspiration and assistance in completing these studies. I would also like to thank my associates and other friends, particularly Ed Suzuki, for helping me keep my perspective.

For Anna and Stephen, a special thanks for being what they are.

Support for this research, provided by the Petroleum Research Fund and National Science Foundation is gratefully acknowledged.

TABLE OF CONTENTS

Chapter		Page
I	INTRODUCTION	1
	Ionic Metal Tetrahydroborates	5
	Covalent Metal Tetrahydroborates	8
	Vibrational Spectra	13
	NMR Spectra	17
II	EXPERIMENTAL	21
	Sample Preparation	21
	Aluminum Tristetrahydroborate	21
	Cyclopentadienylberyllium Tetrahydroborate	24
	Equipment	25
	Vacuum System	25
	Cryogenics	26
	Spectrometers	29
	Sampling	32
III	ALUMINUM TRISTETRAHYDROBORATE	35
	Results and Discussion	36
	Terminal BH Stretches	54
	Bridge BH Stretches	55
	Bridge AlH Stretches	56
	Bending Vibrations	58
	Low Frequency Skeletal Modes	59
	Lattice and Combination Bands	61
	Structural Inferences from the Spectra	62
	Product Rule Calculations	63
	Comparison with Previous Work	66
	NMR - Raman Studies of Liquid $Al(BH_4)_3$	67
	Summary	71
IV	CYCLOPENTADIENYLBERYLLIUM TETRAHYDROBORATE	73
	Results and Discussion	74
	C_5H_5 Ring Vibrations	93
	CH Stretches	99
	CH Bends	100
	CC Motions	103
	Vibrations of the Metal Tetrahydroborate Group	106
	Local Symmetry and Number of Bridging Hydrogens	106
	Terminal BH Stretches	108
	Bridge BH Stretches	110
	Bridge BeH Stretches	110
	Bending Vibrations	111

TABLE OF CONTENTS (Continued)

Skeletal Vibrations 114
Lattice and Combination Bands 121
Product Rule Calculations 122
Structural Inferences from the Spectra 122
Summary 126

BIBLIOGRAPHY 127

LIST OF FIGURES

Figure		Page
1	Formation and stability of metal tetrahydroborates as a function of metal electronegativity (X_M).	4
2	Polymeric chain structure of $Be(BH_4)_2$.	12
3	Effect of the number of bridging hydrogens on the bridge stretching frequencies (cm^{-1}).	15
4	Effect of the number of bridging hydrogens on the terminal stretching frequencies (cm^{-1}).	16
5	System for the preparation of $Al(BH_4)_3$.	23
6	Metal and CsI substrates and dewar used in cryogenic studies.	28
7	Infrared reflection optics for cryogenic studies.	30
8	Infrared and Raman spectra of $Al(BH_4)_3$.	37
9	Infrared and Raman spectra of $Al(BD_4)_3$.	38
10	Infrared and Raman spectra of C_5H_5BeCl.	75
11	Infrared and Raman spectra of $C_5H_5BeBH_4$.	76
12	Infrared and Raman spectra of $C_5H_5BeBD_4$.	77
13	Schematic sketches of the ring, metal tetrahydroborate, and skeletal fundamental vibrations.	92

LIST OF TABLES

Table		Page
1	Elements forming metal tetrahydroborate compounds.	3
2	Some physical properties of ionic tetrahydroborates.	4
3	Group frequencies and activities for the tetrahydroborate ion.	7
4	Some physical properties of $Al(BH_4)_3$.	9
5	Ligand and adduct groups found in common covalent tetrahydroborates.	10
6	Group frequencies for covalent metal tetrahydroborates and tetradeuteroborates (parentheses)(cm^{-1}).	18
7	Sample and substrate solid deposition temperatures.	34
8	Vibrational frequencies (cm^{-1}) of $Al(BH_4)_3$.	39
9	Vibrational frequencies (cm^{-1}) of $Al(BD_4)_3$.	44
10	Symmetry predictions for D_{3h} and D_3 models of $Al(BH_4)_3$.	50
11	Fundamental vibrations (cm^{-1}) of solid aluminum tristetrahydroborate.	64
12	Product rule calculations for aluminum tristetrahydroborate.	64
13	Vibrational frequencies (cm^{-1}) of C_5H_5BeCl.	78
14	Vibrational frequencies (cm^{-1}) of $C_5H_5BeBH_4$.	82
15	Vibrational frequencies (cm^{-1}) of $C_5H_5BeBD_4$.	86
16	C_5H_5 fundamental frequencies (cm^{-1}).	94
17	$BeBH_4$ and $BeBD_4$ fundamental frequencies (cm^{-1}).	95
18	Skeletal frequencies (cm^{-1}).	97
19	Number and symmetry of the hydrogen stretching fundamentals for the possible bridging hydrogen geometries.	107

LIST OF TABLES (Continued)

20 Bond distances, skeletal frequencies, eigenvectors, and force constants for xyz models of relevant molecules. 117

21 Product rule calculations for $C_5H_5BeBH_4$ and $C_5H_5BeBD_4$. 123

INFRARED AND RAMAN VIBRATIONAL STUDIES OF ALUMINUM TRISTETRAHYDROBORATE AND CYCLOPENTADIENYLBERYLLIUM TETRAHYDROBORATE

I. INTRODUCTION

Chemical interest in metal tetrahydroborates stems from their properties as an important class of reducing agents, their unique multiple hydrogen bridge structures (which serve as simple models of three center bonds), and their rapid interchange of terminal and bridging hydrogens (making them some of the most fluxional molecules known). Some of them are also among the most volatile compounds of the metal to which they are bonded, a feature of considerable commercial importance for metal separation processes.

A better understanding of metal tetrahydroborates in relation to the role of the metal atom properties in determining the bridging hydrogen geometries and bonding is clearly desirable. The elucidation of this role depends in part upon the detailed characterization of their vibrational spectra. To this end infrared and Raman spectroscopic studies of aluminum tristetrahydroborate and cyclopentadienylberyllium tetrahydroborate systems were undertaken.

This introduction discusses some of the general physical and chemical properties of metal tetrahydroborates and the relation of these properties to the vibrational and NMR spectra of these tetrahydroborates. In particular, emphasis is placed on the relation be-

tween the multiple hydrogen bridge bonding and the vibrational spectra of the covalent metal tetrahydroborates. Further introductory remarks specific to $Al(BH_4)_3$ and $C_5H_5BeBH_4$ will be found in later chapters dealing with these compounds.

Throughout much of the literature, the term borohydride has been commonly used to refer to the BH_4^- ion bonded to metals. However, based upon a recommendation by the American Chemical Society, and in conformity with use in Chemical Abstracts, the term tetrahydroborate will be used throughout this thesis to designate the BH_4^- ion, whether in solution, ionically bonded, or covalently bridge bonded.

The first metal tetrahydroborate was prepared in 1933 by Stock (1)—— $NaBH_4$. Subsequent work by Schlesinger and co-workers produced $Al(BH_4)_3$ (2), $Be(BH_4)_2$ (3), and $LiBH_4$ (4) in 1940. The metathetic reaction (reaction in the absence of solvent) of the metal halide with either lithium or sodium tetrahydroborate, used by Schlesinger and co-workers, is one of the most useful and general methods of preparing metal tetrahydroborates. The balanced reaction is

$$M(X)_n + n\ YBH_4 \rightleftharpoons M(BH_4)_n + n\ YX\ ,$$

where X = halide, Y = sodium or lithium, and M = metal.

Since then a number of metal tetrahydroborates have been prepared. Those metals for which tetrahydroborates have been prepared are listed in Table 1 (5).

Table 1. Elements forming metal tetrahydroborate compounds. (Asterisks indicate compounds stabilized at room temperature by coordination with phosphine ligands).

Li	Be											
Na	Mg				Al							
K	Ca				(Ga)							
Rb	Sr				(In)	(Sn)						
Cs	Ba				Tl(I)							
	Ti(III)				Cr	(Mn)	(Fe)	(Co)	Ni	(Cu)*	Zn	
Y	Zr(IV)	Nb								(Ag)*	(Cd)	
	Hf(IV)									(Au)		
	La	Sm	Eu	Gd	Tb	Dy	Ho	Er	Tm	Yb	Lu	
	Th					U	Np					

The elements underlined form "simple" tetrahydroborates, i.e., of the general formula $M(BH_4)_x$. Those elements not underlined form stable tetrahydroborates when coordinated to other ligands, while those in parentheses have only been isolated at low temperatures. James and Wallbridge have extensively reviewed the physical and chemical properties of metal tetrahydroborates (5).

The formation and stability of metal tetrahydroborates can be interpreted as a competition between a metal ion and a borane group for a hydride ion. This process is diagrammed in Figure 1.

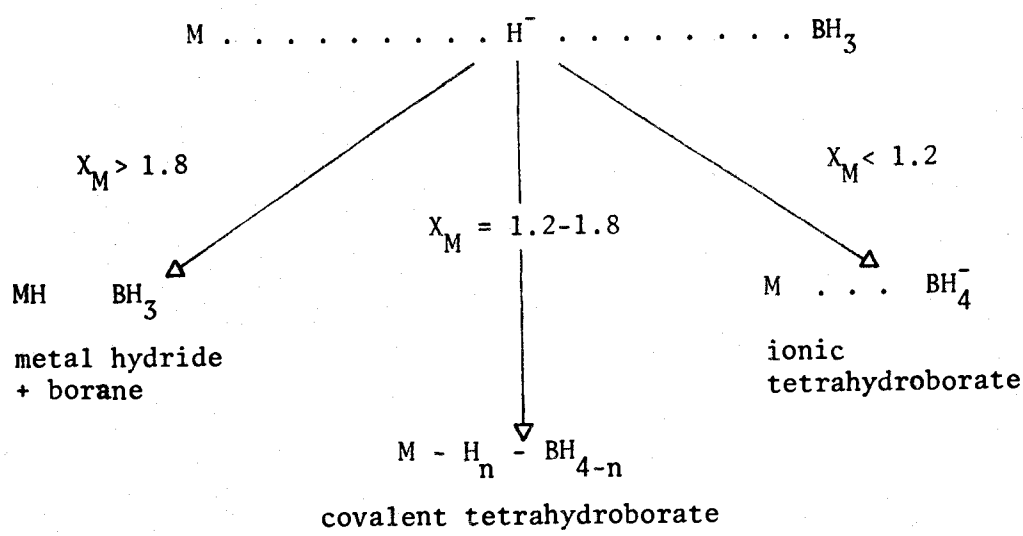

Figure 1. Formation and stability of metal tetrahydroborates as a function of metal electronegativity (X_M).

The increased stability of some metal tetrahydroborates where ligands other than the tetrahydroborate group are attached to the

metal can be explained as a reduction in metal electronegativity as a result of ligand attachment. Metal ions with electronegativities in the range 1.2 to 1.8 form tetrahydroborates which exhibit physical and chemical properties differing widely from tetrahydroborates formed from metal ions with electronegativities less than 1.2. On this basis, the former metal tetrahydroborates have been classified as covalent and the latter as ionic.

Ionic Metal Tetrahydroborates

Ionic tetrahydroborates are characteristically slowly hydrolyzed, are insoluble in non-polar solvents, and have low volatility and high melting points and decomposition temperatures. Table 2 lists some of their physical properties.

Neutron diffraction, X-ray diffraction, infrared studies of the solid state, Raman studies in liquid ammonia, and NMR studies of ionic tetrahydroborates (5) all suggest that the tetrahydroborate ion has tetrahedral symmetry in these compounds. Tetrahydroborate ion vibrational group frequencies and activities (T_d symmetry) are listed in Table 3.

Table 2. Some physical properties of ionic tetrahydroborates (5).

	$LiBH_4$	$NaBH_4$	KBH_4	$RbBH_4$	$CsBH_4$
Melting point, °C	268	505	585	---	---
Decomp. temp., °C	380	315	584	600	600
Density, (g/cm^3)	0.68	1.08	1.17	1.71	2.40
Refractive index	---	1.547	1.490	1.487	1.498
Lattice energy (Kcal/mole)	189.3	166.7	157	155	150.6
Enthalpy of formation $\Delta H°$ (Kcal/mole)	-44.1	-43.8	-58	-59	-63
Entropy, $S°$ (cal/mole °K)	-30.7	-30.2	-38.7	-43.0	-46.0
Structure	ortho-rhombic	fcc	fcc	fcc	fcc
Space group	Pcmn	Fm3m	Fm3m	Fm3m	Fm3m
M-B distance, Å	2.47	3.08	3.36	3.52	3.72

Table 3. Group frequencies and activities for the tetrahydroborate ion.

		H(cm^{-1})	D(cm^{-1})	H/D
BH sym stretch	A_1(R)	2250-2350	1550-1630	1.44
BH asym stretch	F_2(IR,R)	2200-2350	1600-1750	1.35
BH_2 sym bend	E(R)	1150-1350	850-950	1.40
BH_2 asym bend	F_2(IR,R)	1000-1150	800-850	1.31

Covalent Metal Tetrahydroborates

In marked contrast to the ionic tetrahydroborates, the highly volatile covalent tetrahydroborates exhibit low melting points (a number, e.g., $Al(BH_4)_3$ and $C_5H_5BeBH_4$, are liquids at room temperature), low decomposition temperatures, and violent or explosive hydrolysis in air. Some of the physical properties of $Al(BH_4)_3$, which are representative of the physical properties of other covalent tetrahydroborates, are listed in Table 4.

A variety of covalent tetrahydroborates can be prepared (and in some cases only prepared) by replacing one or more of the tetrahydroborate groups with some other ligand or by adding various adducts. Table 5 lists most of the ligand and adduct groups which have been found in the covalent tetrahydroborates which have been reported.

Covalent metal tetrahydroborates are particularly interesting structurally in that the metal and boron atoms are bonded through hydrogen bridges. For the attachment of a single tetrahydroborate group to the metal atom several structures, involving differences only in the number of bridging hydrogens, are possible. These structures may be represented by the following general formula, $M\text{-}H_n\text{-}BH_{4-n}$, where n can equal 1, 2, or 3. Singly bridged structures (n=1) have been observed for $B_2H_7^-$ and $(R_3B)_2H^-$ ($R = CH_3$, C_2H_5) (6,7), which are not strictly metal tetrahydroborates, since the "metal atom" in these

Table 4. Some physical properties of $Al(BH_4)_3$ (5).

Mp, °C	-64.5
Bp, °C	+44.5
Vapor pressure	$\log P_{mm} = 7.808-1565/T$
Heat vaporization (Kcal/mole)	7.16
Trouton constant	22.5
Density (g/cm^3)[a]	$d = 0.7866-0.000793T$
Viscosity (poise)[b]	$n = 23x10^{-5}d^{1/3}e^{1291d/T}$
Surface tension (dyn/cm)[c]	$= (61.0-0.13T)d^{2/3}$
Molar volume (ml/mole)	131.3
ΔH_f (Kcal/mole)[d]	-72.1
ΔH_{hydrol} (Kcal/mole)	-989.1
$\Delta H_{combustion}$ (Kcal/mole)	-196.2
S° (liq) (cal/°K mole)	69.1
C°_p (liq) (cal/°K mole)	46.5

[a] 208.6-274.5°K.

[b] 209.3-305.6°K.

[c] 209.6-305.1°K.

[d] from complete combustion and hydrolysis experiments.

Table 5. Ligand and adduct groups found in common covalent tetrahydroborates.

ligand	adduct
C_5H_5, CH_3CH_2, CH_3,	$(CH_3)_3N$, $(CH_3)_2NH$, CH_3NH_2, NH_3,
CH_3CH_2O, $(CH_3)_3SiO$,	$(CH_3)_2O$, $(CH_3CH_2)_2O$, C_4H_8O, $(CH_3)_2S$,
$(CH_3CH_2)_3SiO$,	$(CH_3)_3P$, $(CH_3)_3As$, $(C_6H_5)_3P$,
LiH, LiH_2, LiH_3,	B_3H_8, $B_{10}H_{13}$
F, Cl	

compounds is boron.

All covalent tetrahydroborates studied so far have exhibited either double or triple hydrogen bridges (n = 2 or 3, respectively). Of these possibilities the double bridged structure is by far the more prevalent. Therefore, in order to list those tetrahydroborates falling into each group it is sufficient to list only those with triple hydrogen bridges: vapor phase $Be(BH_4)_2$ (8,9), vapor and solid phase $U(BH_4)_4$ (10), vapor phase and crystalline $Zr(BH_4)_4$ (11, 12, and 13), vapor phase $Hf(BH_4)_4$ (13), and solid $(C_5H_5)_3ThBH_4$ and $(C_5H_5)_3UBH_4$ (14). Triple hydrogen bridge structures have also been observed for $Hf(BH_4)_4$ (13), $(C_5H_5)_3ThBH_4$, and $(C_5H_5)_3UBH_4$ (14) in benzene solutions.

However, the behavior of $Be(BH_4)_2$ and CH_3ZnBH_4 indicate that a subtle balance is involved. Gaseous $Be(BH_4)_2$ consists of an equilibrium mixture of double and triply bridged structures (8). However, when the mixture is isolated in a matrix, the slightly more stable triply bridged structure is predominantly trapped (8). Upon solidification, $Be(BH_4)_2$ yields polymeric chains of double bridged ions (15,16) (see Figure 2). CH_3ZnBH_4 has also been observed to yield ionic polymeric chains in the solid phase (17).

Considerable chemical interest centers on the role of the metal ion properties (electronegativity, electronic configuration, size, polarizability, etc.) in relation to the multiple hydrogen bridge bonding observed in covalent metal tetrahydroborates. Unam-

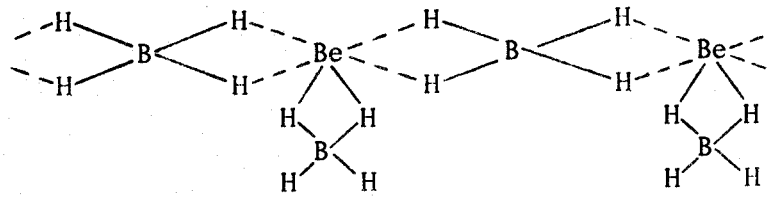

Figure 2. Polymeric chain structure of $Be(BH_4)_2$.

biguous structural information is a necessary prerequisite to a full understanding of these properties. To this end a variety of experimental techniques have been employed.

X-ray, neutron, and electron diffraction methods have been useful in fixing the structure of the heavy metal skeleton, but these techniques are somewhat insensitive to the location of hydrogens near the metal atoms. Similarly, NMR studies are hindered by a terminal, bridging hydrogen exchange process, which is too fast ($\tau \leq 10^{-4}$ sec) (14) to yield structural information on the bridging hydrogens. Vibrational spectroscopy, however, does yield information on the number and relative geometry of the bridging hydrogens.

Vibrational Spectra

The best assignment of the fundamental vibrations in terms of the possible molecular symmetries determines the number and relative geometry of the bridging hydrogens. This assignment is considerably simplified if only a single symmetry need be considered. For covalent metal tetrahydroborates this usually reduces to determining initially whether the molecule is doubly or triply hydrogen bridged. Since the number of infrared and Raman active fundamentals in the boron-hydrogen terminal stretching region (2300-2650 cm^{-1}) and the boron-hydrogen bridge stretching region (1930-2300 cm^{-1}) will generally be different for structures with different numbers of

bridging and terminal hydrogens, the number of bridging and terminal hydrogens is usually readily apparent.

The effect of changes in the number of bridging hydrogens on the boron-hydrogen bridging and terminal stretching frequencies can be seen in Figures 3 and 4 (8), respectively. With increasing number of bridging hydrogens (i.e., as the electronegativity of the metal increases relative to that of boron), the vibrational frequencies associated with motions of the bridging hydrogens split to higher and lower frequencies, reaching in the limit the tetrahydroborate ion stretching and bending frequencies, respectively. This splitting can be alternatively viewed as a strengthening of the BH_b stretches (at the expense of the MH_b stretches), as the boron becomes more electropositive with respect to the metal in their competition for the hydride ion. At the same time the frequencies of the terminal hydrogen stretches are increasing.

The observed fundamentals have been assigned on the basis of group frequency characterization, infrared and Raman activities and frequency coincidences, liquid Raman polarization studies, and isotopic studies. These criteria are often complicated by Fermi-resonance, overtones and combination bands, inherently weak or inactive fundamentals, and crystal splitting. Despite these complications, in instances of high molecular symmetry (e.g., $Al(BH_4)_3$) the above criteria do allow a confident assignment of the fundamental vibrations. For molecules with lower symmetry (e.g., $C_5H_5BeBH_4$) an unam-

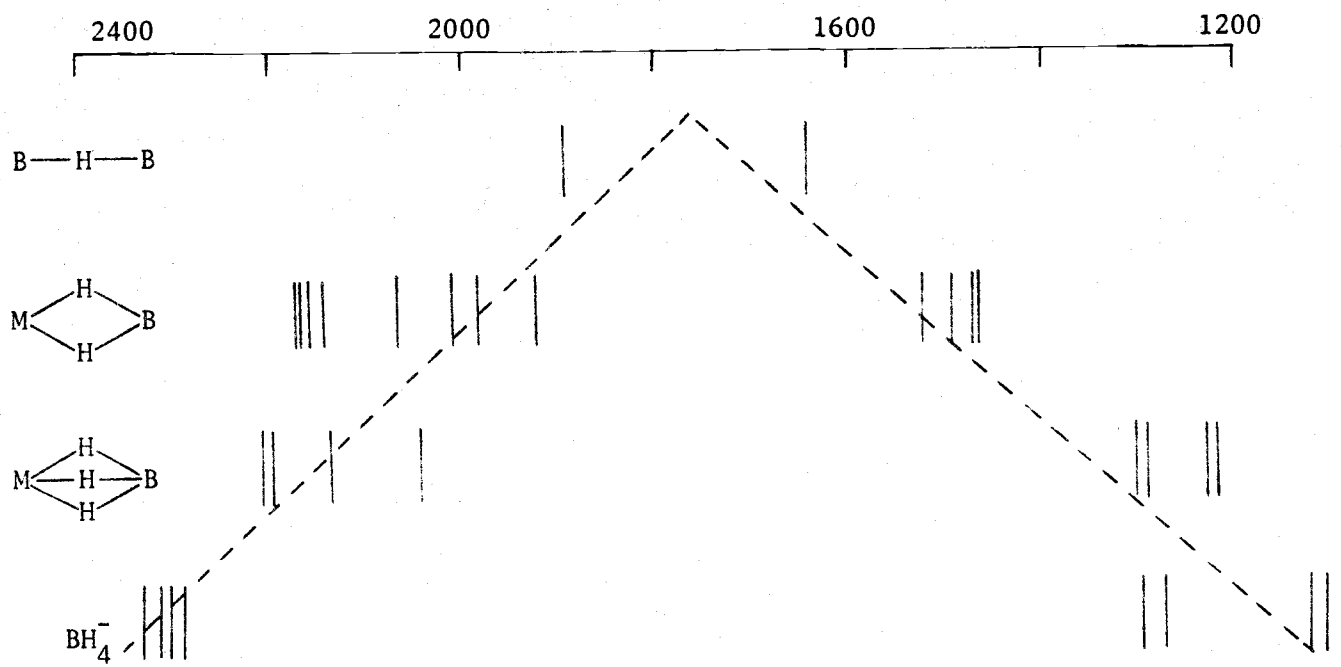

Figure 3. Effect of the number of bridging hydrogens on the bridge stretching frequencies (cm^{-1}).

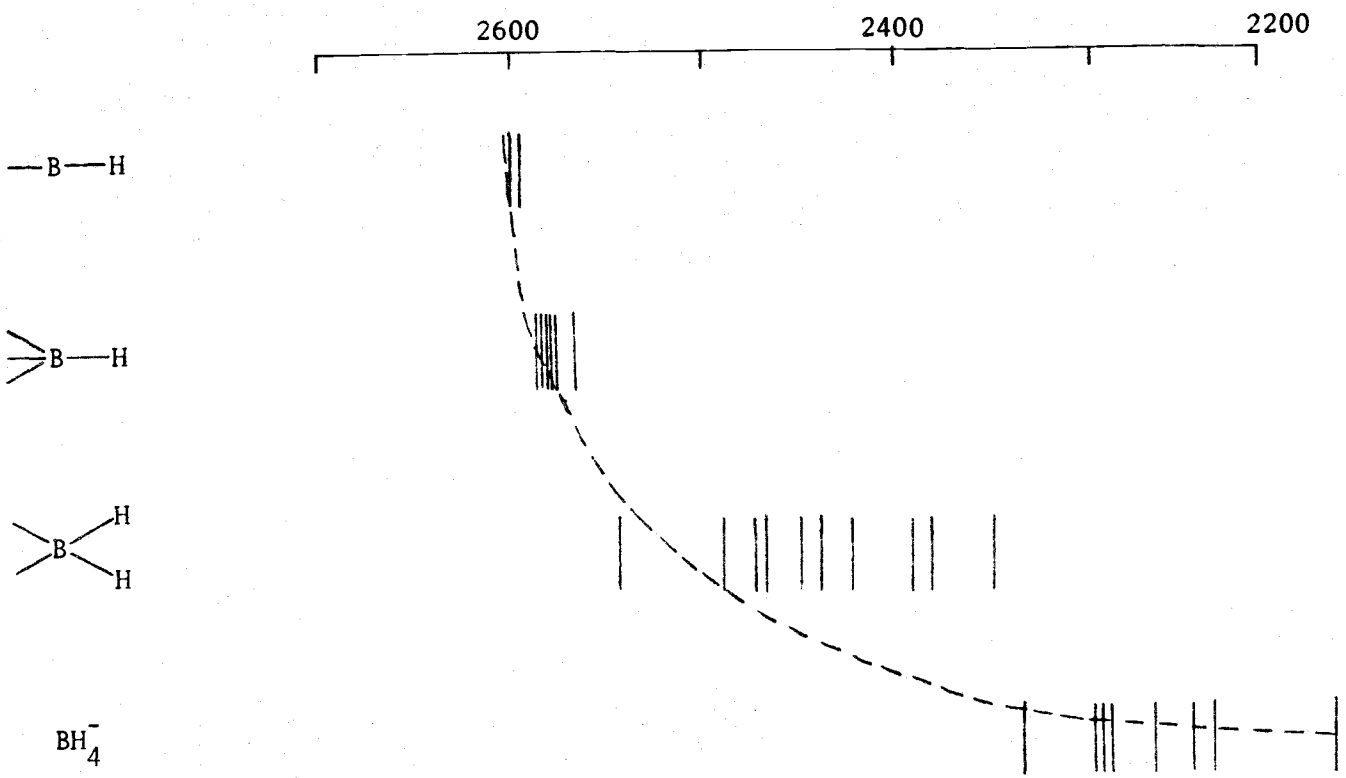

Figure 4. Effect of the number of bridging hydrogens on the terminal stretching frequencies (cm^{-1}).

biguous choice cannot be made and the assignment of the fundamental vibrations rests heavily on previous studies of similar systems.

Table 6 lists the group frequencies for the possible covalent metal tetrahydroborate bridge structures.

Some spectral splitting may result due to the presence of two naturally occurring isotopes of boron, ^{11}B (81.17% relative abundance) and ^{10}B (18.83% relative abundance). Except for those normal modes which predominantly involve boron motion (e.g., the metal-boron stretch), the boron 10,11 isotopic splitting is not normally resolved.

NMR Spectra

Unlike diborane, which exhibits two distinct proton NMR signals, corresponding to the bridging and terminal hydrogens, covalent metal tetrahydroborates exhibit only one signal. This indicates that the bridging and terminal hydrogens in these compounds are equivalent on an NMR time scale. Assuming equivalent terminal and bridging protons, the ^{1}H proton NMR spectrum for $M\text{-}H_n\text{-}BH_{4-n}$, n = 1,2, or 3, coupling with ^{11}B (I = 3/2),yields a quartet with relative intensities 1:1:1:1. Superimposed on this spectrum will be a weaker septet with equal relative intensities due to coupling with ^{10}B (I = 3). The proton NMR spectra are further complicated by coupling to those metals with non-zero nuclear spin (e.g., $Al(BH_4)_3$). The ^{11}B NMR

Table 6. Group frequencies for covalent metal tetrahydroborates and tetradeuteroborates (parentheses) (cm^{-1}).

	single bridge	double bridge		triple bridge	
BH_t sym stretch	2300-2450	2320-2480	(1720-1850)	2450-2640	(1840-1980)
BH_t asym stretch		2360-2540	(1750-1890)		
BH_b stretches	1900-2100	1940-2280	(1560-1890)	2000-2270	(1460-1670)
BH_t deformation	1000-1150	1100-1140	(820-900)	1120-1300	(810-950)
BH_t rock		960-1000	(720-760)		
BH_t wag		740-780	(560-590)		
BH_t twist		1100-1200	(770-850)		

spectrum consists of a quintet with 1:4:6:4:1 relative intensities due to coupling with the four equivalent ^{1}H protons (I = 1/2).

The ^{1}H proton NMR spectra of covalent metal tetrahydroborates will typically show shifts of ∿4 ppm downfield to 2 ppm upfield relative to tetramethylsilane. These shifts are a sensitive function of the metal to which the group is bonded. On the other hand the $J(^{11}B\text{-}H)$ coupling constant is relatively unaffected by the metal atom and ranges from 80 to 90 Hz for most covalent metal tetrahydroborates. This also reflects the equivalency of the terminal and bridging hydrogens.

Considerable controversy surrounds the temperature dependence of the ^{1}H proton NMR spectrum of covalent metal tetrahydroborates which, with increasing temperature, changes from a broad, unresolved band to a quartet consistent with ^{11}B coupling. This observed temperature dependence of the NMR spectra of metal tetrahydroborates has been attributed to: slowing of the bridge-terminal hydrogen exchange process (18-21), virtual decoupling (22), thermal decoupling (23), and the variable rate of ^{10}B and ^{11}B quadrupolar spin-lattice relaxation (14).

In an attempt to clarify some of these anomalies, correlated NMR - Raman spectra of $Al(BH_4)_3$ are discussed in a later chapter. In addition infrared and Raman spectra of $Al(BH_4)_3$ and $C_5H_5BeBH_4$ will be presented and an effort will be made to assign the vibrational fundamentals in each of these compounds in terms of one of the pos-

sible bridging geometries. From these assignments inferences will be drawn concerning the bonding and geometry of the bridging hydrogens in these metal tetrahydroborates.

II. EXPERIMENTAL

Sample Preparation

Aluminum Tristetrahydroborate

In all that follows, except for the nature of the reactants, the preparations of $Al(BH_4)_3$ and $Al(BD_4)_3$ are the same. The text will refer only to $Al(BH_4)_3$.

$Al(BH_4)_3$ was prepared in the metathetic reaction of aluminum trichloride and the corresponding alkali metal tetrahydroborate, following the method of Schlesinger, et.al. (24). The reaction is

$$AlCl_3 + 3NaBH_4 \rightleftharpoons Al(BH_4)_3 + 3NaCl.$$

The sources and number of moles of reactants used in the preparation are as follows:

$AlCl_3$	(anhydrous powder) Mallinckrodt Chemical Works J. T. Baker Chemical Co.	.06 moles
$NaBH_4$	Alpha Inorganics, Inc.	.13 moles
$LiBH_4$	(95 atom % deuterium) Chemische Fabrik, Switzerland	.13 moles

Due to the extreme reactivity of covalent metal tetrahydroborates, certain precautions were observed in their preparation. The preparation was carried out in an air and water free vacuum system and all vacuum seals were lubricated with Kel-F, a fluorocarbon grease. In addition the reactants were added to the reaction flask

in a nitrogen filled dry bag.

Figure 5 describes the system for the preparation of $Al(BH_4)_3$, where a, b, c, d, e, and f are high vacuum stopcocks; g, h, and i are cold traps; j is a mercury bubbler; k is a 500 ml round bottom flask containing glass beads and a stir bar; l is a nitrogen gas inlet; m is a glass wool plug; n is an oil bath; o is a combination hot plate and magnetic stirrer; p is a manometer; q is a thermocouple vacuum gauge; r is the pumping system; and s is a sampling port.

Initially the reaction flask was frozen with liquid nitrogen and the gaseous nitrogen, introduced with the reactants in the nitrogen filled dry bag, pumped off. While stirring and pumping on the reaction mixture, liquid nitrogen was added to the cold traps g, h, and i and the oil bath brought slowly to 130°C. Progress of the reaction was monitored by closing stopcock e and observing any subsequent pressure increase as recorded by the mercury bubbler. After approximately two hours the reaction ceased. The liquid nitrogen in trap i was replaced with a chlorobenzene - liquid nitrogen slush bath (-45°C) and the more volatile products, principally $Al(BH_4)_3$ and B_2H_6, were allowed to condense in trap h. The liquid nitrogen in trap h was then replaced with a 60% ethanol, 40% ether - liquid nitrogen slush bath (-140°C) and B_2H_6 (BP = -92°C) was condensed in trap g. After allowing the contents of trap h to expand into the gas phase, a hexane - liquid nitrogen slush bath (-94°C) was placed on trap h

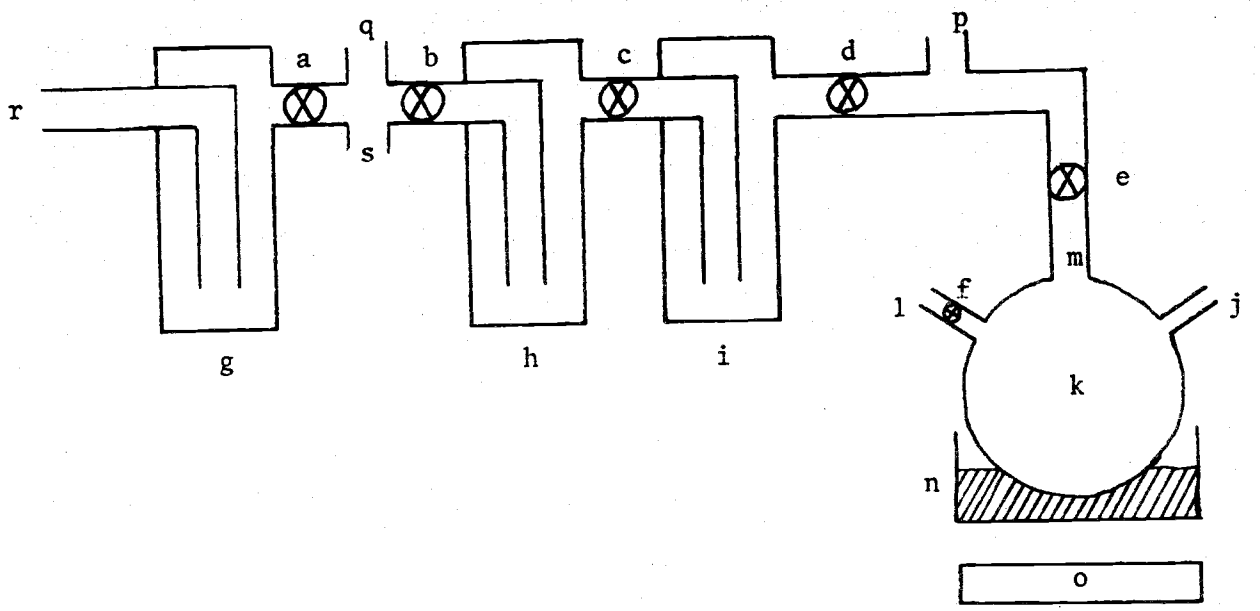

Figure 5. System for the preparation of $Al(BH_4)_3$.

and any remaining non-condensibles were pumped off. With trap h at -63°C (chloroform - liquid nitrogen slush bath) the product, $Al(BH_4)_3$ (Mp = -64°C), was distilled from trap h into a three liter gas storage bulb. The resultant product pressure of 13 torr in the bulb indicated a yield of 5%. For $Al(BD_4)_3$ examination of the Raman intensities of the $Al(BD_4)_2BD_3H$ impurity indicated contamination with hydrogen to be less than 1%.

Cyclopentadienylberyllium Tetrahydroborate

For these studies $C_5H_5BeBH_4$ and $C_5H_5BeBD_4$ were synthesized (25), as outlined below, by Thomas H. Cook (26). In this reaction $(C_5H_5)_2Be$ (Rocky Mountain Research Inc.) and $BeCl_2$ (Alpha Inorganics, Inc.) reacted at 55-60°C for 1-2 hours, yielding upon vacuum distillation colorless crystals of C_5H_5BeCl. Subsequent reaction of C_5H_5BeCl with $LiBH_4$ (Alpha Inorganics, Inc.) at 60°C for 1/2 hour yielded $C_5H_5BeBH_4$. Reaction with $LiBD_4$ (Chemische Fabrik, Switzerland) gave $C_5H_5BeBD_4$. $C_5H_5BeBH_4$ and $C_5H_5BeBD_4$ are colorless liquids at 25°C and, being more volatile than any of the reactants, are easily purified by vacuum distillation. For $C_5H_5BeBD_4$, examination of the Raman intensities of the $C_5H_5BeBD_3H$ impurity indicated contamination with hydrogen to be less than 4%.

Equipment

Vacuum System

The vacuum systems were constructed of metal (stainless steel, copper, and brass) and glass. Couplings and seals were made with a judicious mixture of solder, gyrolock and torrlock "quick" vacuum fittings, Duk seal, and black wax. Standard taper fittings were lubricated with either Apiezon N, a low vapor pressure vacuum grease, or Kel-F, a fluorocarbon grease. In the later work with C_5H_5BeCl, $C_5H_5BeBH_4$, and $C_5H_5BeBD_4$, greaseless stopcocks (Ace Vacuum Incorporated) were used.

The pumping system consisted of a Consolidated Vacuum Corporation (CVC) PMCS-2C high vacuum stainless steel oil diffusion pump and a Cenco Instruments Co. Hyvac-14 mechanical forepump. With low vapor pressure Silicone DC-704 pump oil and a liquid nitrogen cold trap between the diffusion pump and the cell, pressures of 1×10^{-6} torr were routinely achieved. Pressure measurement was accomplished with a Pirani gauge from 1000 to 10^{-3} torr and a Bayard-Alpert type ionization tube from 10^{-3} to 10^{-7} torr. These were connected to a Phillips Model No. 260 002 ionization gauge controller. Calibration was done by direct comparison with other gauges.

Cryogenics

Two types of cryogenic systems were used to achieve the 12 to 25°K temperatures at which the solid and matrix spectra were recorded. On the initial studies of $Al(BH_4)_3$ an Air Products Model AC-3L open-cycle Joule-Thompson refrigerator (27) was used. In this system liquid nitrogen is used to pre-cool high pressure incoming hydrogen gas below its inversion temperature of 202°K, after which further cooling is achieved through expansion of the hydrogen. In exiting from the system this gas passes through a heat exchanger, further cooling the incoming hydrogen. Eventually some of the hydrogen liquefies in a small reservoir in thermal contact with the experimentally accessible substrate. Normally temperatures of 18-22°K could be maintained for 12-20 hours of continuous operation. By varying the back pressure above the liquefied hydrogen the accessible temperature range could be extended beyond the temperature of liquid hydrogen (20°K).

In later studies an Air Products Displex TM closed-cycle Joule-Thompson refrigerator (28) was used. Employing a regenerator (a biased heat exchanger in which heat is removed from the incoming gas, stored, and then given up to the exhausted gas) and a displacer (a piston in which the work of compression is converted to heat by Joule-Thompson expansion and then dissipated in a heat exchanger), this refrigerator uses helium as the working gas in a reversible

Carnot cycle. A small heater increases the useable range of this refrigerator from 12°K to near room temperature.

The substrate on which the matrix or solid sample is deposited consists of either a highly polished hollow aluminum or copper block or a CsI window clamped in a metal frame (see Figure 6). Thermal contact between all separable pieces is provided by indium gaskets greased with Apiezon-N. The experimental load (substrate, sample, and incident radiation) raises the tip temperature 1 to 2 °K.

To eliminate thermal contact of the tip with the room temperature surroundings and to prevent the formation of unwanted condensates, pressures of at least 10^{-5} torr are necessary. These pressures are achieved by placing the tip in an evacuable dewar (see Figure 6). In spite of pumping continuously for 24 hours and heating the walls of the dewar and auxiliary plumbing prior to performing an experiment, solid water could always be detected in the infrared experiments after about ten hours.

Instrumental access to the tip is provided by five windows mounted on the base and sides of the dewar (see Figure 6). Either CsI or polyethylene windows were used in the infrared experiments, while in the Raman experiments glass windows were used. Access to the tip is also provided for thermocouple leads and sample deposition ports. Since rotation of the tip relative to the dewar is possible, more than one deposition and or type of window can be used in a single experiment.

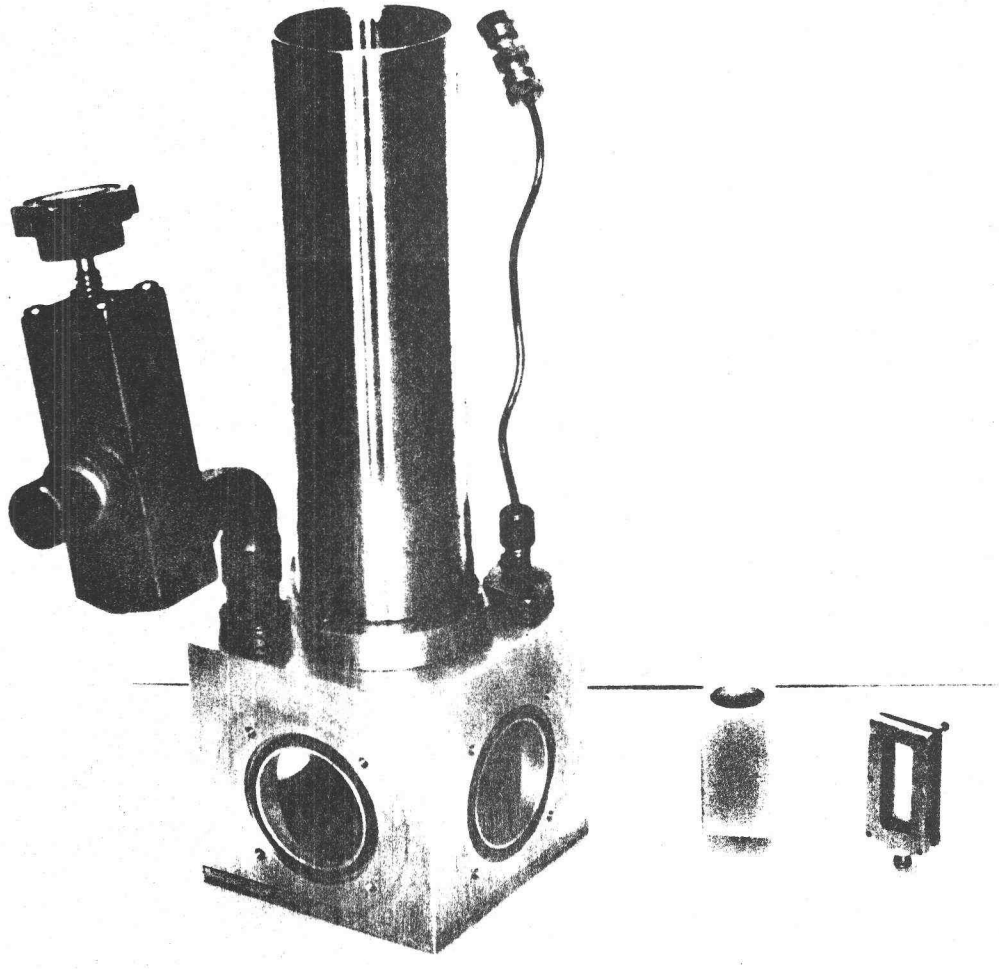

Figure 6. Metal and CsI substrates and dewar used in cryogenic studies.

Temperature measurement from 12 to 300°K is supplied by a chromel-P versus gold - .07% iron thermocouple mounted on the substrate, referenced to ice water, and coupled to a Leeds and Northrup 8686 millivolt potentiometer. On the displex refrigerator additional temperature measurement from 12 to 26°K is provided by an equilibrium hydrogen vapor pressure thermometer. In the course of the experiments the temperature stability was observed to be ± 2°K.

Spectrometers

The initial infrared studies on $Al(BH_4)_3$ were done on a Beckman IR-7 spectrometer, while later studies on $C_5H_5BeBH_4$ were done on a Perkin Elmer 180. The Beckman IR-7 (29) is a foreprism/grating infrared spectrometer employing a Nerst glower source and a thermocouple detector. Capable of .3 cm^{-1} resolution at 1000 cm^{-1}, all high resolution spectra taken with this instrument were recorded at a resolution of 1 cm^{-1}. The spectrometer was calibrated with atmospheric water vapor.

The Perkin Elmer 180 (30) is a double beam grating infrared spectrometer, employing an air cooled globar source and a thermopile detector. All spectra were recorded at 1 cm^{-1} resolution throughout the 180 to 4200 cm^{-1} range of the spectrometer. High resolution spectra of HCl, DCl, HCN, DCN, H_2O, CO_2, and CH_4 were used to calibrate the instrument. These spectrometers were used exclusively in

the double beam mode. Differences in atmospheric path length in the two beams, due to placement of the cell in the sample beam, often resulted in detection of atmospheric CO_2 and water vapor.

Within the infrared sampling cavities two sampling schemes were employed: the more conventional transmittance mode and a reflectance mode (31), the latter offering several advantages over the transmittance mode in cryogenic studies (see Figure 7).

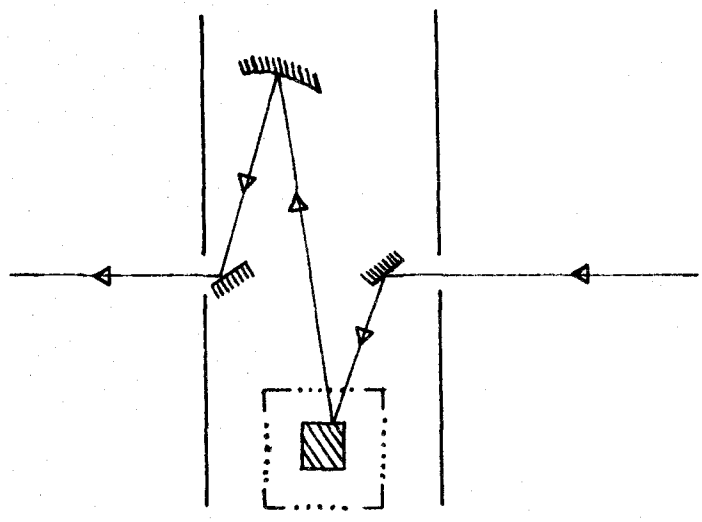

Figure 7. Infrared reflection optics for cryogenic studies.

Although approximately 10% less energy throughput is available in the reflectance mode when compared to the transmittance mode, other considerations make it the preferable sampling scheme. Some of these are:

1. Deposition times are halved, since the beam traverses the sample twice.
2. Rotation of the substrate relative to the deposition and sampling ports, allows four separate experiments to be run without warming up. In principle, any combination of four different window materials and four different deposits should be possible in a given run. In practice, however, vacuum couplings inhibit the rotation of the dewar and at most two types of window materials are available.
3. The higher thermal conductivity of the aluminum substrate, as compared to the CsI substrate, gives better isolation for matrix deposits.
4. In experiments where reaction with the aluminum substrate may be a problem, a platinum surface may be deposited on the aluminum.

All Raman studies were done on a Cary 82 Raman Spectrometer. A Coherent Radiation Laboratories Model 52B argon-ion laser provided the incident radiation (principally the 5145 Å and 4880 Å lines) used in these studies. This radiation is first passed through a set of filter optics, sacrificing one-half the incident intensity, to remove the numerous plasma lines associated with each laser line. The incident radiation is then focused at the sampling point and 90% of the scattered radiation collected at 90° by the spectrometer's fl collection optics. The scattered radiation is dispersed by three

successive monochromators. This last feature results in negligible Rayleigh scattered radiation reaching the phototube and allows Raman spectra to be recorded to within 10 - 50 cm^{-1} of the exciting frequency. Measurement of the depolarization ratio, $\rho = I_{\perp}/I_{\parallel}$, was accomplished by first passing the linearly polarized incident radiation through a quarter wave plate, where for $I_{\perp}$ the incident plane of polarization is rotated 90° and for $I_{\parallel}$ the incident plane of polarization is conserved. The scattered radiation was then passed through an analyzer, which accepts only radiation whose plane of polarization is parallel to the plane of polarization of the incident radiation.

^{1}H and ^{11}B NMR spectra of $Al(BH_4)_3$ and $Al(BD_4)_3$ were recorded between -60°C and +80°C on a Varian HA-100 instrument using a conventional temperature controller. All spectra were referenced externally to benzene.

Sampling

All infrared spectra of gaseous samples were taken in standard ten cm Pyrex gas cells fitted with CsI windows (transparent to infrared radiation from 200 - 4000 cm^{-1}).

Raman spectra of liquids were for the most part taken of samples contained in Kimax capillaries. However, for the correlated NMR - Raman studies of liquid $Al(BH_4)_3$ and $Al(BD_4)_3$ and for the Raman

studies of liquid C_5H_5BeCl ($25°C < Mp < 50°C$), NMR tubes were used. For Raman studies in which temperature variation of the sample between -100°C and +100°C was required, a Harney - Miller type cell was used. Heating or cooling in this cell is achieved by flowing either hot or cold nitrogen past the sample tube contained in a transparent dewar. Temperature stability of ±.1°C was achieved as measured on a chromel - alumel thermocouple, referenced to ice water.

Spectra of $Al(BH_4)_3$ and $Al(BD_4)_3$, matrix isolated in argon at a mole ratio of 1 in 500, were obtained in an effort to resolve overlapping gas and liquid phase bands. The samples, premixed in argon in a one liter gas bulb, were deposited at 20±2°K on a CsI or aluminum substrate and then annealed to approximately one-half the sublimation temperature of argon (35°K). Deposition rates, which varied from .05 to .5 millimoles per hour, were controlled using Hoke needle valves and were monitored on a Manostat Corporation Predictability flowmeter.

Infrared and Raman spectra of annealed polycrystalline films at 14 to 20°K were taken to establish coincident infrared and Raman frequencies and to resolve broad gas and liquid phase bands. The samples were deposited at temperatures at which they had vapor pressures of a few torr. During deposition the substrate was kept at a temperature at which annealing could be expected to occur. Table 7 lists the sample and substrate temperatures at which the solid samples were deposited. Complications associated with vibrational studies of

molecules in the solid state, e.g., crystal splitting and changes in activity due to reduction of symmetry, were assumed to be negligible.

To remove any volatile impurities prior to sampling, a vacuum of 10^{-4} torr was applied to the samples, which were maintained at temperatures at which they had vapor pressures less than 10^{-3} torr (-100°C for $Al(BH_4)_3$ and $Al(BD_4)_3$, -78°C for C_5H_5BeCl, $C_5H_5BeBH_4$, and $C_5H_5BeBD_4$).

Table 7. Sample and substrate solid deposition temperatures.

	Sample Temperature (°C)	Substrate Temperature (°C)
$Al(BH_4)_3$	25	-100
$Al(BD_4)_3$	25	-100
C_5H_5BeCl	0	- 45
$C_5H_5BeBH_4$	-20	- 73
$C_5H_5BeBD_4$	-20	- 73

III. ALUMINUM TRISTETRAHYDROBORATE

Electron diffraction studies of gaseous $Al(BH_4)_3$ (32) have shown the AlB_3 framework to be planar with double hydrogen bridges, but the twist angle (θ) of each BH_4 tetrahedron about the AlB bond is uncertain. The diffraction results gave a D_3 structure with $\theta = 17°$, but the authors were not able to rule out a prismatic D_{3h} configuration in which the terminal BH_2 bonds lie in the heavy atom plane ($\theta = 0°$). Similarly, a definite choice between D_3 and D_{3h} structures was not possible from two earlier spectroscopic investigations. These consist of a low resolution vapor phase infrared (IR) study of $Al(BH_4)_3$ in 1949 by Price (33) and a liquid Raman experiment on $Al(^{11}BH_4)_3$, $Al(^{10}BH_4)_3$, $Al(^{11}BD_4)_3$, and $Al(^{10}BD_4)_3$ in 1960 by Emery and Taylor (34). The latter authors gave a partial vibrational assignment based on an assumed D_{3h} structure. Some question exists about the liquid phase, however, since several proton NMR studies of $Al(BH_4)_3$ have shown unusual temperature dependent effects, and it has been suggested that these might be due to the formation of $Al_2B_4H_{18}$ dimers (20) or, possibly, to the existence of two different monomer structures (19).

Because of its high volatility and chemical behavior $Al(BH_4)_3$ serves as a covalent prototype for the doubly bridged compounds and its vibrational spectrum and assignments are important in discussing the spectra and structures of other metal tetrahydroborates. Accord-

ingly, the IR and Raman spectra of several phases of aluminum tris-tetrahydroborate have been obtained with the following objectives in mind:

1. To determine whether the structure changes significantly in going from the vapor to the liquid to the solid phase, as has been observed for $Be(BH_4)_2$ (8) and CH_3ZnBH_4 (17).
2. To obtain high resolution IR spectra from 4000 to 200 cm^{-1} for both $Al(BH_4)_3$ and $Al(BD_4)_3$.
3. To obtain IR and Raman spectra of the same phase to aid in establishing frequency coincidences.
4. To obtain matrix or solid spectra to aid in resolving overlapped gas and liquid phase bands.
5. To use this data to confirm and extend the vibrational assignments of Emery and Taylor and, if possible, to distinguish between a D_{3h} and a D_3 structure.

All of these objectives have been achieved, and the results are reported here along with some observations from correlated NMR - Raman studies of liquid $Al(BH_4)_3$ at various temperatures.

Results and Discussion

The vibrational spectra of various phases of $Al(BH_4)_3$ and $Al(BD_4)_3$ are displayed in Figures 8 and 9, and the corresponding frequencies are listed in Tables 8 and 9. Comparison of the gas,

Figure 8. Infrared and Raman spectra of $Al(BH_4)_3$.

A. IR spectrum - vapor phase at 25°C. Upper trace is 11 mm $Al(BH_4)_3$ in 10 cm cell with CsI windows.

B. IR spectrum - Ar matrix at 25°K, --- = B_2H_6.

C. IR spectrum - solid film at 18°K.

D. Raman spectrum - solid film at 18°K.

E. Raman spectrum - liquid phase at -60°C.

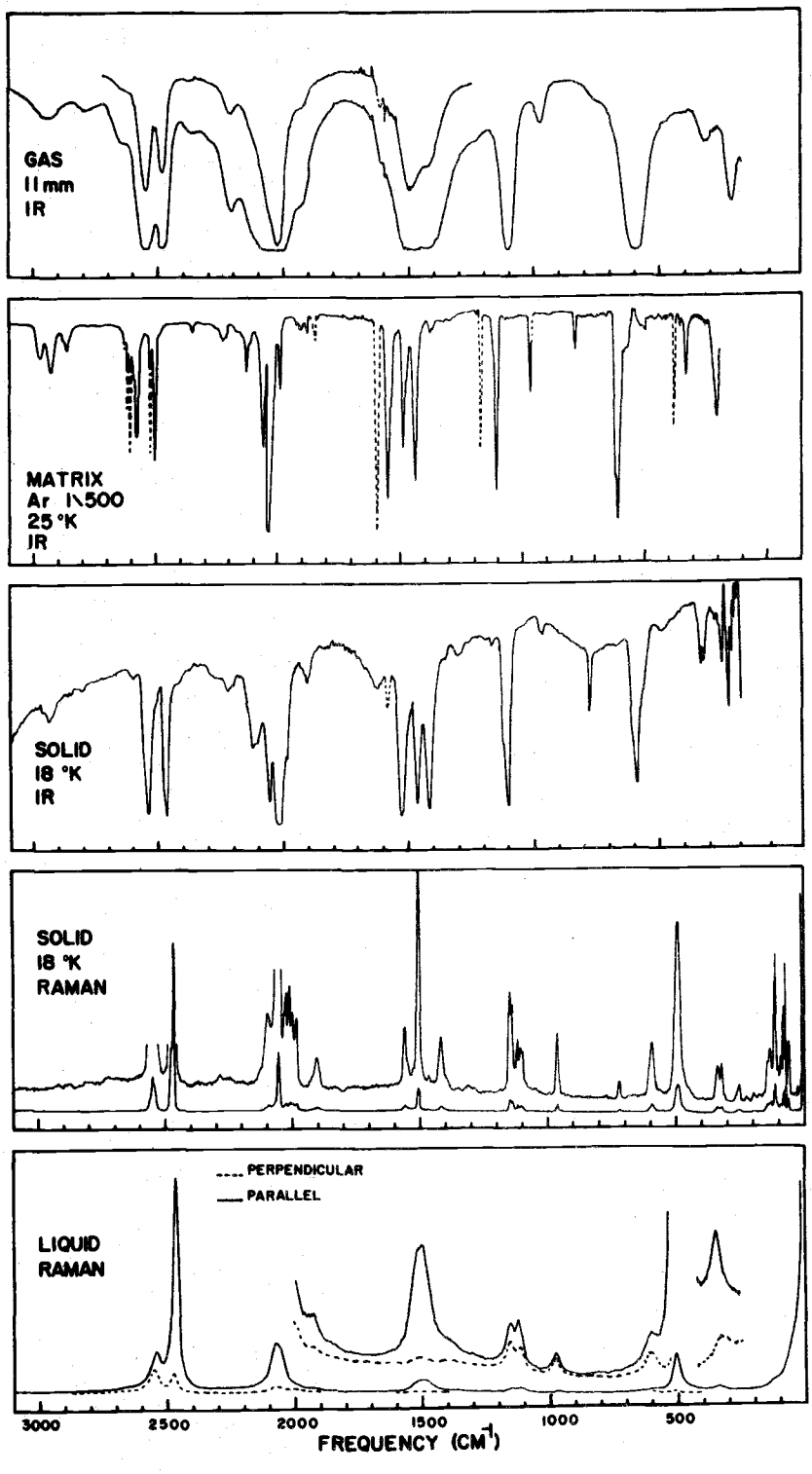
GAS
11mm
IR
MATRIX
Ar 1\500
25 °K
IR
SOLID
18 °K
IR
SOLID
18 °K
RAMAN
PERPENDICULAR
PARALLEL
LIQUID
RAMAN
3000
2500
2000
1500
1000
500
FREQUENCY (CM⁻¹)

Figure 9. Infrared and Raman spectra of $Al(BD_4)_3$.

A. IR spectrum - vapor phase at 25°C. Upper trace is 11 mm $Al(BD_4)_3$ in 10 cm cell with CsI windows.

B. IR spectrum - Ar matrix at 18°K, --- = B_2D_6.

C. IR spectrum - solid film at 14°K.

D. Raman spectrum - solid film at 14°K.

E. Raman spectrum - liquid phase at -60°C.

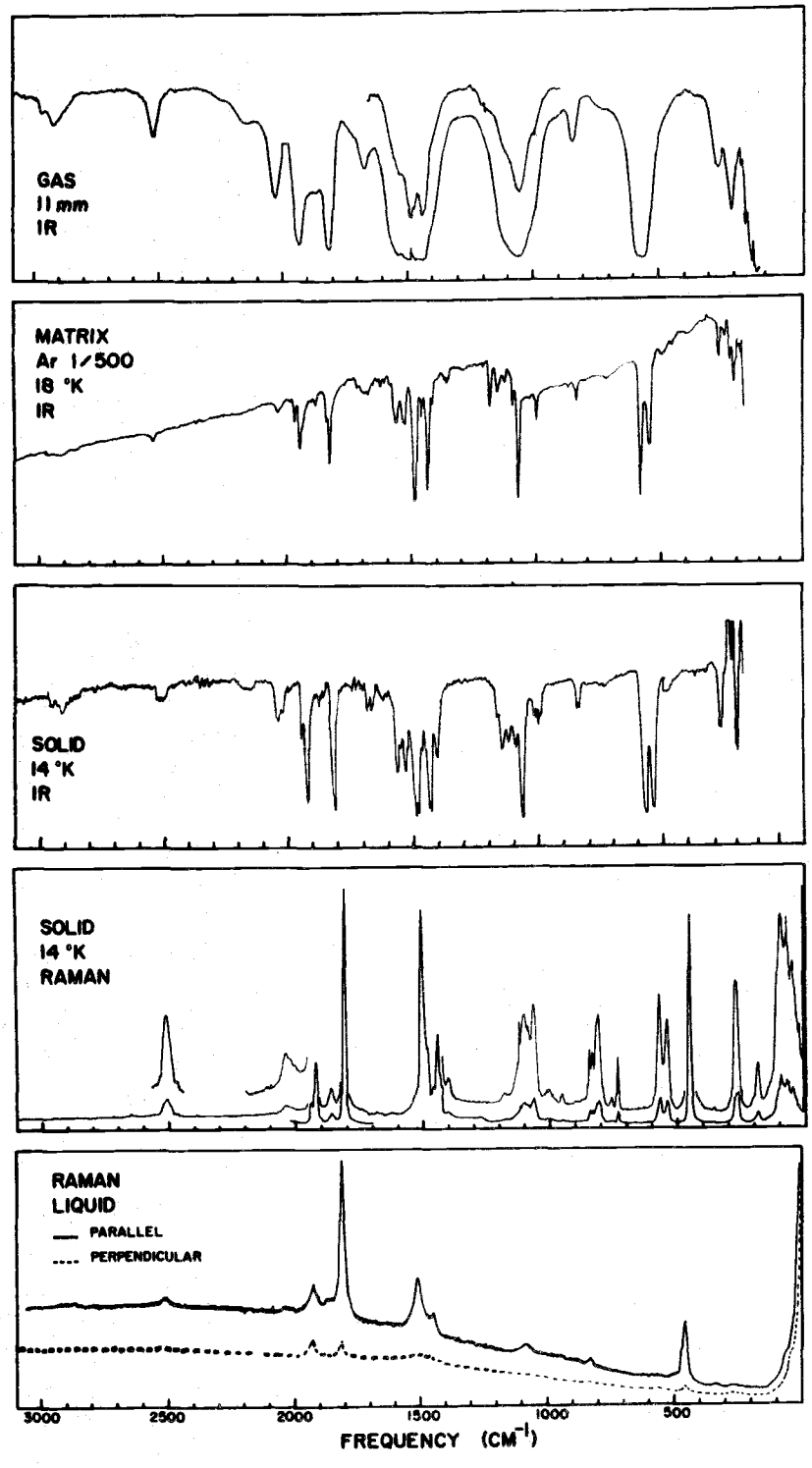
GAS
11 mm
IR
MATRIX
Ar 1/500
18 °K
IR
SOLID
14 °K
IR
SOLID
14 °K
RAMAN
RAMAN
LIQUID
PARALLEL
PERPENDICULAR
3000
2500
2000
1500
1000
500
FREQUENCY (CM⁻¹)

Table 8. Vibrational frequencies (cm^{-1}) of $Al(BH_4)_3$.

Infrared			Raman				
Gas 25°C	Ar Matrix 25°K	Solid 18°K	Solid 18°K	Liquid -60°C	Polarization		Assignment
4020 vw						E'	$\nu_{16} + \nu_{25} = 4034$
3924 w		3940 w				E'	$\nu_{15} + \nu_{18} = 3965$
	2968 w					E'	$\nu_5 + \nu_{16} = 2964$
2940 w,b	2933 m	2939 w				E'	$\nu_3 + \nu_{18} = 2931$
	2860 w					E'	$\nu_{15} + \nu_{22} = 2869$
2790 w,b		2811 vw				E'	$\nu_{13} + \nu_{24} = 2809$
2650 m,sh						E'	$\nu_2 + \nu_{21} = 2655$
	2590 w	2560 s,sh	2565 s,sh			A_2'',E''	$\nu_{18} + \nu_{27} = 2567$
	2579 m,sh						$\nu_{15} - {}^{10}B^{11}B_2$
2555 vs,b	2574 s	2544 vs	2547 s,sh	2550 s	dp	E'	ν_{15}
			2553 vs			A_1'	$\nu_2 + \nu_5 = 2554$
			2484 vs,sh			E'	$\nu_3 + \nu_{20} = 2478$

Table 8. Vibrational frequencies (cm^{-1}) of $Al(BH_4)_3$. (Continued)

Infrared			Raman				
Gas 25°C	Ar Matrix 25°k	Solid 18°K	Solid 18°K	Liquid -60°C	Polarization		Assignment
	2506 m,sh	2476 m,sh	2476 vs,sh				$\nu_{16} - {}^{10}B^{11}B_2$
2490 vs	2501 s	2469 vs	(2471)			E'	ν_{16}
			2471 vvs	2475 vs	P	A_1'	ν_1
		2290 vw	2290 vw	2290 vvw	P	A_1',E'	$\nu_{25} + \nu_{28} = 2288$
2218 s	2230 vw	2225 w				E'	$\nu_4 + \nu_{19} = 2217$
		2199 w				E'	$2\nu_{19} = 2208$
2135 vw,sh	2129 m	2125 m				A_2''	$\nu_{20} + \nu_{26} = 2122$
		2106 m,sh	2192 m			E'	$\nu_3 + \nu_{21} = 2107$
	2070 m,sh					E'	$\nu_{19} + \nu_{20} = 2071$
	2056 s	2059 s	(2059)			E'	ν_{17}
			2059 vs	2075 vs	P	A_1'	ν_2
			2030 m			E''	ν_{24}
2030 vs,b	2027 vs	2026 vs				A_2''	ν_{11}

Table 8. Vibrational frequencies (cm^{-1}) of $Al(BH_4)_3$. (Continued)

Infrared			Raman				
Gas 25°c	Ar Matrix 25°K	Solid 18°K	Solid 18°K	Liquid -60°C	Polarization		Assignment
		2014 s,sh	2017 m	2000 m,sh	dp	E'	$\nu_{18} + \nu_{21} = 2017$
			2004 m			A_1'	$\nu_3 + \nu_5 = 2006$
	1990 m	1985 m,sh	1987 m			E'	$\nu_9(882) + \nu_{19}$,?
				1925 m,sh	P	A_1'	$2\nu_{20} = 1934$
1930 m,sh	1914 vw	1907 w	1907 w			E'	$\nu_5 + \nu_{18} = 1916$
			1565 m			E"	ν_{25}
1505 vs	1547 vs	1531 vs				A_2''	ν_{12}
			1511 vs	1503 s	P	A_1'	ν_3
	1485 s	1468 s				A_2''	$\nu_{22} + \nu_{26} = 1480$
			1471 vw			E"	$\nu_{22} + \nu_{27} = 1471$
1425 s,sh	1438 vs	1419 m	1422 s	1386 m,sh	dp	E'	ν_{18}
		1358 vw	1358 vvw			E'	$\nu_{19} + \nu_{23} = 1359$

Table 8. Vibrational frequencies (cm^{-1}) of $Al(BH_4)_3$. (Continued)

Infrared			Raman				
Gas 25°C	Ar Matrix 25°K	Solid 18°K	Solid 18°K	Liquid -60°C	Polarization		Assignment
		1306 w	1312 vw			A_2'',E''	$\nu_{21} + \nu_{28} = 1319$
			1155 m	1155 m	dp	E''	ν_{26}
			1146 m			E''	ν_{27}
	1120 w,sh	1124 m,sh	1123 w			E'	$\nu_9(868) + \nu_{23}$,?
			1113 w	1124 m	P	A_1'	ν_4
1112 vs	1107 vs	1103 vs	1105 w	1114 m	dp	E'	ν_{19}
981 w	966 vw,sh	966 w	968 w	979 w	dp	E'	ν_{20}
765 w,sh	786 w	799 m				A_2''	ν_{13}
			727 w				ν_{28} - $^{10}B^{11}B_2$
			723 w	~700 vw,sh	dp	E''	ν_{28}
				662 vw	P	A_1'	$2\nu_{22}$ = 650
605 vs	601 vs	595 s	598 m	601 m	dp	E'	ν_{21}

Table 8. Vibrational frequencies (cm^{-1}) of $Al(BH_4)_3$. (Continued)

Infrared			Raman				
Gas 25°C	Ar Matrix 25°K	Solid 18°K	Solid 18°K	Liquid -60°C	Polarization		Assignment
		566 m,sh				E'	$\nu_{22} + \nu_{23} = 580$
			495 vs	512 s	P	A_1'	ν_5
		487 vw				E'	$\nu_{10}(232) + \nu_{23}$?
		337 w	343 w			E'	$\nu_{23} + \nu_L(83)=338$
324 m	332 m	324 w	327 w	320 w	dp	E'	ν_{22}
		254 vw	256 w			E'	ν_{23}
222 m		229 w				A_2''	ν_{14}
			230 vw				ν_L
		216 w					ν_L
		205 w	201 vw				ν_L

ν_L = Lattice Vibration. Additional lattice modes were observed in the Raman spectrum of the solid at at 146 m, 136 m, 120 m, 112 m,sh, 105 m, 95 m, 83 s, 66 m, 61 s, 34 w, 20 m, ?.

Table 9. Vibrational frequencies of (cm^{-1}) of $Al(BD_4)_3$.

Infrared			Raman				
Gas 25°C	Ar Matrix 18°K	Solid 14°K	Solid 14°K	Liquid -60°C	Polarization		Assignment
2965 vw		2950 vw				A_2''	$\nu_1 + \nu_{12} = 2961$
2920 w		2913 vw,b				E'	$\nu_3 + \nu_6 = 2914$
			2652 vw	2655 vw	P	A_1'	$\nu_1 + \nu_4 = 2664$
2522 m	2540 vw	2518 vw,b	2513 m	2512	P		$(BD_4)_2AlD_2BDH$
2151 w						E'	$\nu_3 + \nu_{18} = 2168$
2035 s	2038 vw	2042 m	2045 w	2030 w,sh	P		$(BD_4)_2AlDHBD_2$
		2021 w,sh				A_2''	$\nu_5 + \nu_{11} = 2021$
		1944 m	1948 m			E'	$\nu_5 + \nu_{17} = 1941$
1939 vs	1950 s	1923 vs	1928 vs	1930 m	dp	E'	ν_{15}
	1886 vw	1873 vw	1870 w	1863 w	P		$(BD_4)_2AlD_2BDH$
		1819 vs,sh					$\nu_{16} - {}^{10}B^{11}B_2$
1821 s	1832 s	1812 vs	(1814)			E'	ν_{16}

Table 9. Vibrational frequencies of (cm^{-1}) of $Al(BD_4)_3$. (Continued)

Infrared			Raman				
Gas 25°C	Ar Matrix 18°K	Solid 14°K	Solid 14°K	Liquid -60°C	Polarization		Assignment
			1820 vs,sh				$\nu_1 - {}^{10}B^{11}B_2$
			1814 vvs	1814 vs	P	A_1'	ν_1
		1684 w	1688 vw			E'	$\nu_4 + \nu_{19} = 1687$
			1673 vvw	1670 vvw	P	A_1'	$2\nu_{19} = 1674$
1655 m	1673 vw	1667 w				A_2''	$\nu_3 + \nu_{13} = 1676$
	1565 m	1567 s				A_2''	ν_{11}
				1565 vvw,sh		E''	ν_{24}
1525 vs,sh	1527 m	1533 s					$(BD_4)_2AlDHBD_2$
			1509 vs	1518 s	P	A_1'	ν_2
1476 vvs	1486 vvs	1487 vvs	1486 w	1500 m	dp	E'	ν_{17}
	1462 m	1465 w	1468 vw				$(BD_4)_2AlDHBD_2$
			1447 s	1459 m	P	A_1'	$2\nu_{20} = 1470$
1428 vvs	1435 vs	1433 vvs	1432 w			E'	$2\nu_{20} = 1470$

Table 9. Vibrational frequencies of (cm^{-1}) of $Al(BD_4)_3$. (Continued)

Infrared			Raman				
Gas 25°c	Ar Matrix 18°K	Solid 14°K	Solid 14°K	Liquid -60°C	Polarization		Assignment
1387 s,sh	1417 w,sh	1405 s	1406 w	1400 vvw,sh	dp	A_2'',E''	$\nu_{19} + \nu_{28} = 1409$
	1362 vw,b					E'	$\nu_3 + \nu_{22} = 1372$
			1183 w			E''	ν_{25}
1168 m	1159 m	1147 s				A_2''	ν_{12}
	1135 w	1118 s					$(BD_4)_2AlDHBD_2$
			1102 m,b	1093 w	P	A_1'	ν_3
1105 s,sh	1097 m	1089 s	1088 w,sh			E'	$2\nu_{21} = 1084$
1065 vs,b	1074 vvs	1065 vvs	1068 m	~1070 vw,sh	dp	E'	ν_{18}
		1017 m				A_2''	$\nu_5 + \nu_{13} = 1026$
1005 s,sh	1000 m	1006 m	1008 vw	1000 vvw	dp	A_2'',E''	$\nu_{23} + \nu_{26} = 1007$
		998 m				E'	$\nu_{20} + \nu_{22} = 1005$
		990 m				E'	$\nu_5 + \nu_{21} = 996$
			956 vw	960 vvw			$(BD_4)_2AlD_2BDH$

Table 9. Vibrational frequencies of (cm^{-1}) of $Al(BD_4)_3$. (Continued)

Infrared			Raman				
Gas 25°C	Ar Matrix 18°K	Solid 14°K	Solid 14°K	Liquid -60°C	Polarization		Assignment
			850 w	827 w	P	A_1'	ν_4
	847 vw,sh	844 m				A_2''	$\nu_{22} + \nu_{28} = 842$
851 m	840 w	837 m	838 w	818 w	dp	E'	ν_{19}
			813 m			E''	ν_{26}, ν_{27}
			764 vw			E''	$\nu_{13} + \nu_{23} = 768$
		733 vvw	737 m	742 vw	dp	E'	ν_{20}
575 vvs	580 vvs	574 vvs				A_2''	ν_{13}
			572 m	568 vw	dp	E''	ν_{28}
	554 s	541 vvs	543 m			E'	ν_{21}
			454 vs	465 s	P	A_1'	ν_5
		277 m,sh	278 m,sh				$\nu_{22} - {}^{10}B^{11}B_2$
270 m	275 m	268 m	271 s	274 vw	dp	E'	ν_{22}
216 s	214 s	205 vs				A_2''	ν_{14}

Table 9. Vibrational frequencies (cm^{-1}) of $Al(BD_4)_3$. (Continued)

Infrared			Raman			
Gas 25°C	Ar Matrix 18°K	Solid 14°K	Solid 14°K	Liquid -60°C	Polarization	Assignment
			194 m	190 vvw	dp E'	ν_{23}

Additional lattice vibrations were observed in the Raman spectrum of the solid at 115 s, 102 vs, 81 m, 72 s, 55 s, 30 w.

matrix, and solid IR spectra and the liquid and solid Raman spectra shows only minor frequency shifts in the different phases. Thus it may be concluded that $Al(BH_4)_3$ retains its covalently bonded structure in all phases. (Possible complications in the liquid spectra are discussed later.)

Table 10 summarizes the group theoretical predictions for the D_3 and D_{3h} models, and it is apparent that the activities of the $2A_1''$, $3A_2'$, and 5E" vibrations form the basis for distinction between the two structures. Although active for a D_3 model, the A_1'' and A_2' vibrations are expected to have low intensity, comparable to that of overtone and combination bands, and hence there were doubts that these modes could be clearly assigned. However, the 5E" modes are Raman allowed, and a careful search for them in the infrared spectrum might lead to a more definite statement regarding the structure than was possible from the previous data. This presumes that a confident assignment of the spectra can be made and, to aid in this task, an approximate description of the normal modes of vibration is offered in Table 11. These vibrations are ordered in terms of (roughly) characteristic group frequencies, an arrangement which provides a convenient outline for the discussion of assignments given below. Unless otherwise noted, the vibrational frequencies cited in the discussion will refer to solid $Al(BH_4)_3$ and the corresponding $Al(BD_4)_3$ values will be given in parentheses. For convenience, the number and symmetry of each mode is given in terms of

Table 10. Symmetry predictions for D_{3h} and D_3 models of $Al(BH_4)_3$.

D_{3h}			D_3		
Activity	# Modes	Symmetry	Symmetry	# Modes	Activity
R(P)	5	A_1'	A_1	7	R(P)
—	2	A_1''			
—	3	A_2'	A_2	7	IR
IR	4	A_2''			
R,IR	9	E'	E	14	R,IR
R	5	E''			

Table 11. Fundamental vibrations (cm^{-1}) of solid aluminum tristetrahydroborate.

	Symmetry[a]		Mode					
	D_{3h}	D_3	(D_{3h})	$Al(BH_4)_3$		$Al(BD_4)_3$		ν_H/ν_D
Terminal BH Stretches								
sym.	A_1'	A_1	ν_1	2471	(2473)[b]	1814	(1810)[b]	1.362
sym.	E'	E	ν_{16}	2469	(2493)	1812	(——)	1.363
asym.	A_2'	A_2	ν_8	----	(----)	----	(----)	----
asym.	E'	E	ν_{15}	2544	(2549)	1925	(1928)	1.322
Bridge BH Stretches								
sym.	A_1'	A_1	ν_2	2059	(2069)	1509[c]	(~1500)	1.364
sym.	E'	E	ν_{17}	2059	(2010)	1487[c]	(——)	1.385
asym.	A_2''	A_2	ν_{11}	2026	(2154)	1567	(——)	1.293
asym.	E''	E	ν_{24}	2030	(——)	1565[d]	(——)	1.297
Bridge AlH Stretches								
sym.	A_1'	A_1	ν_3	1511	(1495)	1102	(1092)	1.371
sym.	E'	E	ν_{18}	1420	(~1521)	1066	(——)	1.332

Table 11. Fundamental vibrations (cm^{-1}) of solid aluminum tristetrahydroborate. (Continued)

	Symmetry[a] D_{3h}	D_3	Mode (D_{3h})	$Al(BH_4)_3$		$Al(BD_4)_3$		ν_H/ν_D
Bridge AlH Stretches								
asym.	A_2''	A_2	ν_{12}	1531[c]	(——)	1147	(——)	1.335
asym.	E''	E	ν_{25}	1565	(——)	1183	(——)	1.323
Bends								
BH_2 deformation	A_1'	A_1	ν_4	1113	(1116)	850	(829)	1.309
BH_2 deformation	E'	E	ν_{19}	1104	(1116)	837	(829)	1.319
BH_2 twist	A_1''	A_1	ν_7	----	(----)	---	----	----
BH_2 twist	E''	E	ν_{26}	1155	(——)	813	(——)	1.421
bridge twist	A_1''	A_1	ν_6	----	(----)	----	(----)	----
bridge twist	E''	E	ν_{27}	1146	(1149)	813	(829?)	1.410
BH_2 rock-in plane	A_2'	A_2	ν_9	----	(----)	----	(----)	----
BH_2 rock-in plane	E'	E	ν_{20}	967	(1392)	735	(——)	1.316
BH_2 wag-out of plane	A_2''	A_2	ν_{13}	779	(978)	574	(——)	1.357
BH_2 wag-out of plane	E''	E	ν_{28}	723	(976)	572	(743)	1.264

Table 11. Fundamental vibrations (cm^{-1}) of solid aluminum tristetrahydroborate. (Continued)

Skeletal Modes	Symmetry[a] D_{3h}	Symmetry[a] D_3	Mode (D_{3h})	$Al(BH_4)_3$		$Al(BD_4)_3$		ν_H/ν_D
sym. AlB stretch	A_1'	A_1	ν_5	495	(510)	454	(463)	1.090
asym. AlB stretch	E'	E	ν_{21}	596	(602)	542	(569)	1.100
AlB_3 bend-in plane	E'	E	ν_{22}	325	(318)	270	(267)	1.204
bridge bend	A_2'	A_2	ν_{10}	----	(----)	----	(----)	----
bridge bend	E'	E	ν_{23}	255	(——)	194	(——)	1.314
AlB_3 bend-out of plane	A_2''	A_2	ν_{14}	229	(——)	205	(——)	1.117

[a] All A type modes are in phase; all E modes are out of phase. Mode numbering as in reference 34.

[b] Values in parentheses are previous assignments for gas and liquid phase from reference 34.

[c] These fundamental frequencies are believed to be shifted by Fermi Resonance.

[d] Liquid value.

a D_{3h} model.

Terminal BH Stretches

Four normal modes are expected and these can be viewed as in phase and out of phase combinations of the symmetric (ν_1-A_1', ν_{16}-E') and asymmetric (ν_8-A_2', ν_{15}-E') BH stretches. ν_1 is clearly identified as the strong 2471 (1814) cm^{-1} Raman band since the corresponding liquid feature is polarized. Because ν_1 is not IR active for either D_3 or D_{3h} symmetry, the strong IR band at 2469 (1812) cm^{-1} must be assigned as the E' mode ν_{16}. The negligible splitting between ν_1 and ν_{16} implies that there is very little coupling between the isolated BH_2 groups. The asymmetric stretches are expected to lie at higher frequencies, and the strong IR-Raman feature at 2544 (1925) cm^{-1} is logically assigned as the E' mode ν_{15}. The D_{3h} inactive A_2' counterpart would be IR active for D_3 symmetry, but no clear candidate for this mode could be discerned. This absorption is expected to occur very near 2544 (1925) cm^{-1}, however, and could be buried under ν_{15} if allowed. Assuming $\nu_8 \approx \nu_{15}$, it is worth noting that the average [2507(1869)cm^{-1}] of the four fundamentals lies very near the value of 2515 (1871) cm^{-1} observed for the 'uncoupled' BH(BD) stretch of $(BD_4)_2AlD_2BDH$ which is present as an impurity in the $Al(BD_4)_3$.

Bridge BH Stretches

These four modes can also be characterized as in phase and out of phase combinations of the symmetric (ν_2-A', ν_{17}-E') and asymmetric (ν_{11}-A", ν_{24}-E") BH_2 bridge stretches. From the liquid polarization results, ν_2 is assigned at 2059 (1509) cm^{-1}. In the absence of any significant coupling between the different bridges, the out of phase E' counterpart should be close to ν_2 in frequency and the IR - Raman feature at 2059 (1487) cm^{-1} is thus assigned as ν_{17}. If this choice for ν_{17} is correct, the remaining intense IR feature at 2026 cm^{-1} must be chosen as the A_2" asymmetric stretch ν_{11}. On the basis of intensities, the $Al(BD_4)_3$ frequency for ν_{11} would seem to be the strong IR feature at 1433 cm^{-1}, but, in fact, this is believed to be an E' combination band in Fermi resonance with ν_{17} at 1487 cm^{-1}. Instead, the band at 1567 cm^{-1} is assigned as ν_{11} because this choice resolves a difficulty with the A_2" product rule (vide infra). Also, this reversal of the order of the symmetric and asymmetric BH_b stretches in going from the hydride to the deuteride parallels the observations for $H_2BH_2Be^+$ (ν_{sym} = 2119, ν_{asym} = 2084 cm^{-1}) and $D_2BD_2Be^+$ (ν_{sym} = 1503, ν_{asym} = 1557 cm^{-1}). Finally, as shown below, this choice is more consistent with the frequencies assigned to the the uncoupled bridge stretches of $(BD_4)_2AlDHBD_2$.

There remains the E" asymmetric stretch, ν_{24}, which could be any of the medium Raman bands at 2030, 2017, 2004, or 1987 cm^{-1}. A

slight preference can be established for the 2030 cm^{-1} feature since this is closest to ν_{11} at 2026 cm^{-1} and, moreover, this choice yields an average of the four BH_b fundamental of 2044 cm^{-1}. Although perhaps somewhat fortuitous, this average exactly coincides with the uncoupled BH_b stretch observed at 2044 cm^{-1} for $(BD_4)_2AlDHBD_2$. For solid $Al(BD_4)_3$, ν_{24} was not identified, but it is expected to occur near ν_{11} at 1567 cm^{-1}, and this region is somewhat obscured by the very intense Raman ν_2 mode at 1509 cm^{-1}. When the intensity of ν_2 is reduced for liquid $Al(BD_4)_3$ at -60°C by scanning in the perpendicular polaroid orientation, a weak shoulder does appear at 1565 cm^{-1}. With this value for ν_{24}, the average of the four BD_b stretches occurs at 1532 cm^{-1}, again coincident with an IR feature at 1533 which is assigned as the uncoupled BD_b stretch of $(BD_4)_2AlDHBD_2$.

Bridge AlH Stretches

For each of the bridging BH stretches there is an analogous AlH stretch of the same symmetry. Although these modes will mix somewhat, this coordinate description is preferred to that of Emery and Taylor who designate the bridge BH and AlH stretches as ring stretches and expansions similar to those in diborane. B_2H_6, with four equivalent BH bridge bonds (1.34 Å), does not appear to be a good model for $Al(BH_4)_3$ (and other metal tetrahydroborates) since the AlH bridge bond (1.80 Å) is much longer than the BH bridge bond (1.28 Å). Thus, the

four strongly coupled bridge vibrations for B_2H_6 (2104, 1880, 1768, and 1606 cm^{-1}) can be expected to uncouple when one of the borons is replaced by an aluminum atom, yielding two BH stretches above 2000 cm^{-1} and two AlH stretches below 1600 cm^{-1}.

The A_1' in phase symmetric AlH stretch, ν_3, is easily assigned as the polarized Raman band at 1511 (1102) cm^{-1} and the E' out of phase counterpart, ν_{18}, must be the intense IR - Raman feature at 1420 (1066) cm^{-1}. The E" out of phase asymmetric stretch, ν_{25}, seems logically placed at 1565 (1183) cm^{-1}, the only remaining strong Raman line in this region. For the A_2'' in phase motion, ν_{12}, the intense IR absorption at 1531 (1147) cm^{-1} is preferred over the weaker alternative at 1468 (1089) cm^{-1}. The latter is thought to be an A_2'' overtone, $\nu_{22} + \nu_{26} = 1480$ cm^{-1}, in Fermi resonance with ν_{12} at 1531 cm^{-1}. In support of this assignment, it may be noted that the average of the four AlD stretches, 1124 cm^{-1}, is very close to the 1118 cm^{-1} band attributed to the uncoupled Al-D stretch in $(BD_4)_2AlDHBD_2$. (The corresponding average for $Al(BH_4)_3$, 1507 cm^{-1}, could not be distinguished because of intense $Al(BD_4)_3$ features in this region.) From the frequency differences between the in phase and out of phase AlH stretches, it is apparent that coupling through the common central atom is significant. This implies that an AlH stretch-stretch interaction force constant will be important in any force constant calculations for $Al(BH_4)_3$.

Bending Vibrations

Ten bending modes are expected in the region 1300 to 600 cm^{-1}, and these are perhaps the most difficult fundamentals to assign. The eight bending motions of the terminal BH_2 groups can be described as in phase and out of phase motions involving deformations (ν_4-A_1', ν_{19}-E'), twists (ν_7-A_1'', ν_{26}-E''), in plane rocks (ν_9-A_2', ν_{20}-E'), and out of plane wags (ν_{13}-A'', ν_{28}-E''). Since little coupling is expected between different BH_2 groups, it can be anticipated that the in phase and out of phase frequencies will be similar in value. On this basis, the polarized Raman band at 1113 (850) cm^{-1} and the IR - Raman feature at 1104 (837) cm^{-1} are assigned as ν_4 and ν_{19} respectively. Similarly the A_2'' IR absorption at 779 (574) cm^{-1} and the E'' Raman line at 723 (572) cm^{-1} can be attributed to the wagging modes ν_{13} and ν_{27}. Only one other E' mode, ν_{20}, is expected in the bending region and the IR - Raman feature at 967 (735) cm^{-1} seems to be the most logical choice since no combination mode of the correct symmetry can readily explain this band. The corresponding in phase rock, ν_9, is IR active for a D_3 structure, but no other IR absorptions were observed in this region.

There remains the A_1'' in phase and E'' out of phase BH_{2t} and bridge twisting fundamentals. The BH_{2t} twist, ν_{26}, can be associated with the medium Raman band at 1155 (813) cm^{-1} which does not appear in the IR. For $Al(BH_4)_3$ there is another medium Raman feature at

1146 cm^{-1} which is also clearly absent in the IR. Efforts to explain this as an E" or A_1' combination band were not successful and hence this feature is tentatively assigned as ν_{27}, the E" bridge twist. Although an $Al(BD_4)_3$ feature for this mode is not clearly resolved, both ν_{26} and ν_{27} may contribute to the rather broad band at 813 cm^{-1}. Some support for this is found in the large H/D ratios that this gives for both E" vibrations (1.41). [This follows from the fact that the product rule predicts average H/D ratios of 1.37, 1.32, 1.30, and 1.27 for the E", A_1', E', and A_2" modes respectively (see later)]. The principal misgiving about this bridge twist assignment is that the frequency seems too high for the twisting of the rather weak bridge bonds. It is conceivable that the E" mode at 723 cm^{-1} is more properly termed the bridge twist, but this would yield rather different values for the two wags (A_2" = 779, E" = 1146 cm^{-1}). Since there does not seem any doubt that the A_2" band is correctly assigned, the assignments given in Tables 8 and 9 represent the favored choice. One additional alternative involving the inactive A_1" twists will be mentioned later.

Low Frequency Skeletal Modes

Six low frequency modes are anticipated in the region below 600 cm^{-1}. The symmetric AlB_3 stretch, ν_5, is assigned as the polarized A_1' Raman band at 495 (454) cm^{-1} while the IR - Raman feature

at 596 (542) cm^{-1} is logically chosen to be ν_{21}, the E' asymmetric stretch. Treating the BH_4 units as point masses, approximate H/D ratios of 1.12 and 1.06 are calculated for ν_1 and ν_{21}, in rough agreement with the observed values of 1.09 and 1.10. The A_2'' out of plane bend, ν_{14}, appears in the IR at 229 (204) cm^{-1}, giving a H/D ratio of 1.12. This value is noticeably larger than a calculated value of 1.06, indicating that hydrogen motion is important in this vibration.

The other three low frequency modes consist of an E' in plane AlB_3 bend (ν_{22}) plus an A_2' in phase (ν_{10}) and E' out of phase (ν_{23}) bridge bend. In B_2H_6 the bridge bend appears at 368 (250) cm^{-1}, and it involves primarily hydrogen motion (H/D = 1.47). In $Al(BH_4)_3$ this mode is expected to be lower in frequency because of the longer, weaker bridge bonds and hence the IR - Raman feature at 255 (194) cm^{-1} is chosen as ν_{23}. The lower H/D ratio of 1.31, compared to B_2H_6, is reasonable since this mode will mix significantly with the E' AlB_3 in plane bend. The latter is assigned as the IR - Raman band at 325 (270) cm^{-1} and the relatively high H/D ratio (1.20) for this bend is also in accord with the idea of substantial mixing. The remaining A_2' bridge bend would be IR active for a D_3 configuration, and it is conceivable that this could be attributed to a weak IR feature at 337 (277) cm^{-1}. However, this frequency seems high in comparison to the out of phase bridge bend at 255 cm^{-1} and the H/D ratio also seems too low (1.22). Moreover, the 337 cm^{-1} feature

disappears in the matrix spectrum and hence it could be due to crystal splitting of ν_{22}, to a combination involving lattice modes or, for the 277 band, to a $^{10}B^{11}B_2$ isotopic shoulder of ν_{22}.

Lattice and Combination Bands

A number of low frequency Raman modes were observed which are attributed to translational and librational motions in the unit cell. Since the crystal structure of $Al(BH_4)_3$ is unknown, little can be said about these modes, although it is worth noting that the number of Raman lattice bands for $Al(BH_4)_3$ (~13) implies that the unit cell must contain at least four molecules.

A number of features were assigned as combinations or overtones of the observed fundamentals, as indicated in Tables 8 and 9. In some cases, several alternative assignments exist; those listed were chosen on the basis of frequency fit and intensities of the parent fundamentals. Only a few bands (indicated by ? in the tables) were not easily assigned as binary combinations of observed fundamentals. Of these, $Al(BH_4)_3$ frequencies at 1986, 1124, and 487 cm^{-1} can be explained as combinations involving the inactive fundamentals ν_9 and ν_{10}. If correct, these assignments would place the in phase BH_2 rock, ν_9, at 882 ≈ 868 cm^{-1} (to be compared with the out of phase rock at 967 cm^{-1}) and the in phase bridge bend, ν_{10}, at 323 cm^{-1} (out of phase value = 255 cm^{-1}). Although these values are reasonable,

the evidence for them is minimal and other possible assignments of the active fundamentals have been considered. However, none of these seem quite as satisfactory and, in general, the present accounting of the combination bands is taken as support for the fundamental assignments.

Structural Inferences from the Spectra

Table 11 summarizes the assignments of the fundamental vibrations of aluminum tristetrahydroborate, and it is seen that all the D_{3h} allowed fundamentals are tentatively identified. Assuming that the structure is significatnly distorted to D_3, one would anticipate the following:

1. The three A_2' fundamentals would become IR active. Of these the BH stretch, ν_8, would surely be lost under the E' mode ν_{15}. The BH_2 rock, ν_9, would be expected to lie between 1300 and 700 cm^{-1}, but there does not appear to be any likely candidate for either $Al(BH_4)_3$ or $Al(BD_4)_3$. The remaining mode, the bridge bend, ν_{10}, could be a feature at 337 (277) cm^{-1} but, as mentioned above, reasonable alternatives can explain this absorption.
2. The two A_1'' twisting fundamentals would become Raman active. Possible candidates for $Al(BH_4)_3$ include Raman bands at 1146 and 727 cm^{-1}, while features at 956, 813, and 764 cm^{-1} occur in

the $Al(BD_4)_3$ spectrum. The 1146 (813) cm^{-1} combination could conceivably be the A_1'' BH_2 twist rather than the E" bridge twist as presently assigned, but the evidence for this is not compelling.

3. The five E" Raman modes would become IR active also. The present assignment places these fundamentals at 2030 (1565), 1565 (1183), 1153 (813), 1146 (813) and 723 (572). For $Al(BH_4)_3$ the IR spectrum near the 1565, 1155, 1146, and 723 cm^{-1} regions is reasonably uncluttered, yet no trace of any of these bands was detected. Similarly, for $Al(BD_4)_3$ there is no indication of either the 1183 or 813 cm^{-1} fundamentals even though these IR regions are also clear.

Most of the above observations represent evidence of a negative kind and hence some caution is advisable in reaching structural conclusions. Despite this comment, the present work provides the best experimental indication currently available that the structure is D_{3h} or, if D_3, that the configuration is only minimally distorted from D_{3h}.

Product Rule Calculations

The D_{3h} structural parameters from the electron diffraction work (32) yield the inertial moments listed in Table 12 for $Al(^{11}BH_4)_3$ and $Al(^{11}BD_4)_3$. The resultant theoretical product rule factors are

Table 12. Product rule calculations for aluminum tristetrahydroborate.

Moments of Inertia[a]		$Al(^{11}BH_4)_3$	$Al(^{11}BD_4)_3$
I_z	(Amu-Å^2)	217.02	282.38
$I_x = I_y$	(Amu-Å^2)	115.56	155.24
M	(Amu)	72.11	84.19
Product Rule Factor			
A_1':	$(D/H)^2$	3.996	3.638
A_1'':	$(D/H)^1$	1.999	----
A_2':	$(D/H)^{3/2}\ [I_z(H)/I_z(D)]^{1/2}$	2.478	----
A_2'':	$(D/H)^{3/2}\ [M(H)/M(D)]^{1/2}$	2.616	2.616
E':	$(D/H)^{7/2}\ [M(H)/M(D)]^{1/2}$	10.452	10.028
E'':	$(D/H)^{5/2}\ [I_x(H)/I_x(D)]^{1/2}$	4.875	4.343

[a] D_{3h} structural parameters taken from reference 8.

also shown for each symmetry species, along with the observed results. The agreement is reasonable in view of the fact that anharmonicity usually yields an observed factor which is lower than the theoretical result. In addition, no correction has been made for frequency shifts due to Fermi resonance of several fundamentals [e.g., for $Al(BH_4)_3$, a resonant pair occurs at 1531-1468 (A_2'' while for $Al(BD_4)_3$, resonance is suspected at 1509-1447 (A_1' and 1487-1433 (E')]. Such corrections would raise the observed A_1' and E' factors slightly while lowering the A_2'' factor a small amount.

With regard to the frequency assignments, the product rule predictions were of particular value in assigning ν_{11}, the A_2'' BH bridge stretch. Of the five A_2'' vibrations, only for ν_{11} were there several alternatives: 2125/1667 = 1.275, 2125/1567 = 1.356, 2026/1567 = 1.293, or 2026/1433 = 1.414. Of these, the second and fourth can be rejected because they produce an observed A_2'' product factor which is <u>greater</u> than the theoretical value. Of the other two alternatives, the third is preferred because it is more consistent with minimal coupling between the different BH bridges and it also gives average BH and BD frequencies coincident with the uncoupled values observed for $(BD_4)_2AlDHBD_2$. It may also be noted that any alternate choice of the E'' twisting modes ν_{26} and ν_{27} would probably give a poorer Product Rule result since the present assignment involves H/D ratios of 1.41 and, if anything, the observed ratio is on the low side.

Comparison with Previous Work

From gas phase IR spectra of $Al(BH_4)_3$ and liquid Raman spectra of $Al(BH_4)_3$ and $Al(BD_4)_3$, Emery and Taylor have previously assigned 17 of the 23 observable fundamentals of $Al(BH_4)_3$ and 11 of 23 for $Al(BD_4)_3$. Their results are listed in Table 11 along with the present values for all 46 frequencies. Comparison of the common assignments shows differences for five fundamentals: A_2'' (ν_{11}, ν_{13}), E' (ν_{18}, ν_{20}) and E'' (ν_{28}). The basis for choosing ν_{11} = 2026 cm^{-1} rather than 2154 cm^{-1} has already been discussed. The assignment of the other A_2'' mode (ν_{13} = 779 cm^{-1}) is also not doubted for the following reasons. First, a careful search showed no trace of this mode in the Raman spectrum of the solid and hence the A_2'' label seems justified. Since the feature is observed at 18°K, it cannot be assigned as a difference band and the only A_2'' combination mode below 1200 cm^{-1} would be much too low ($\nu_5 = \nu_{14}$ = 724 cm^{-1}). Inasmuch as the 779 cm^{-1} feature is also observed in the gas and in the matrix, it cannot be due to a combination involving the lattice modes; thus, the conclusion that it is ν_{13} seems firm.

If ν_{13} = 779 cm^{-1}, another explanation is required for the 976 cm^{-1} feature assigned as ν_{13} by Emery and Taylor. In fact, this band appears also in the Raman spectrum, and Emery and Taylor choose to view this as an accidental degeneracy between ν_{13} (A_2'') and ν_{28} (E''). This frequency is labeled as the E' fundamental ν_{20} instead

since, within experimental accuracy, the rather sharp solid phase IR and Raman peaks are coincident at 967 (735) cm^{-1}. Moreover, the 967 cm^{-1} is viewed as a more reasonable value for this E' rocking mode than is the value of 1392 cm^{-1} assigned by Emery and Taylor. (In B_2H_6 the rocks occur at 950 and 920 cm^{-1}, in $H_2BH_2Be^+$ at 970 cm^{-1}.) The 1392 band is preferably assigned as the E' symmetric AlH stretch, ν_{18}, a value which is not inconsistent with the other AlH stretching modes near 1500 cm^{-1}. In fact, Emery and Taylor assigned ν_{18} to a weak Raman feature at 1521 cm^{-1}, which has gone undetected in this study despite a careful search in both the solid phase and in the liquid at -60°C (the low temperature yields narrower liquid Raman lines and hence greater resolution). Thus, the 1521 cm^{-1} band is felt to be spurious and the present assignments are preferred for all five fundamentals in question.

NMR - Raman Studies of Liquid $Al(BH_4)_3$

There have been two detailed NMR studies of $Al(BH_4)_3$ each yielding slightly different results. In 1955, Ogg and Ray (20) found a broad proton resonance of about 300 cps width which sharpened to a quartet on heating. They interpreted this in terms of an equilibrium between $2Al(BH_4)_3$ (broad signal) $\rightleftharpoons$ $Al_2B_4H_{18}$ (sharp signal) + B_2H_6 with the dimer form the dominant species at 80°C. Maybury and Ahnell (19) later reexamined the NMR spectrum from -40

to +90°C and found evidence for two different monomeric species of $Al(BH_4)_3$. The first of these (I) gave a broad NMR spectrum on condensation from the vapor phase and, when heated rapidly to 90°C, reversibly gave a quartet; observations similar to those of Ogg and Ray. However, prolonged heating at 25-90°C seemed to produce a "modified" species (II) which showed the broad to sharp spectral conversion (still reversible) at a much lower temperature (~-20°C) than I (~40°C). From these observations they speculated that I and II might be due to D_{3h} and D_3 structures respectively, and they attributed the appearance of the quartet spectrum at higher temperatures to rotation of the BH_4 groups rather than to the presence of $Al_2B_4H_{18}$. This rotation was presumed to spin-spin decouple the protons and the ^{27}Al nucleus which broadens the spectrum due to the large Al quadrupole moment. It is not entirely clear that this is the case, however, since Marks and Shimp (14) have recently shown that similar spectral changes in the NMR spectra of $Zr(BH_4)_4$ and $Hf(BH_4)_4$ are due to the variable rate of boron quadrupolar spin lattice relaxation. These authors conclude that BH_4 reorientation is rapid even at -80°C for these molecules, and it may well be that a similar situation obtains for $Al(BH_4)_3$.

In an effort to clarify the situation in the liquid phase, several NMR - Raman experiments were carried out for $Al(BH_4)_3$. In one experiment, 0.5 cc of $Al(BH_4)_3$ was condensed from the vapor phase in an NMR tube, sealed off under vacuum, and a Raman spectrum was re-

corded at room temperature. An NMR spectrum was recorded two days later which was characteristic of Maybury and Ahnells' form II since the broad to sharp spectral conversion occurred at ~-10°C. This result was somewhat surprising since Maybury and Ahnell reported that 6-8 weeks were required for the I→II conversion at 25°C. In view of this observation a second NMR sample was freshly prepared in a similar manner and, prior to a Raman scan, NMR spectra were immediately taken which were identical to those obtained in the first experiment.

Raman spectra were also recorded for both samples from -60 to +60°C, but, other than a slight broadening of all bands at the higher temperatures, no significant spectral changes were observed. However, on heating the samples to 80°C for several hours, very weak, polarized features grew in at 2315, 905, 795, 380, and 270 cm^{-1}, and these remained on cooling to 25°C. Accompanying this change, a trace of solid white residue of unknown composition formed on the NMR tube above the liquid level. It should be stressed that the total extent of reaction was very small, as judged by the amount of the white residue and the intensity of the strongest new band at 795 cm^{-1} (~equal in intensity to the weak $Al(BH_4)_3$ feature at 979 cm^{-1}). An NMR spectrum taken of this sample was similar to that obtained prior to heating to 80°C except that the quartet was noticeably sharper at room temperature.

A number of possible explanations for these observations have

been considered, and the simplest one, which is favored, is that a "catalytic" product is produced in the thermal decomposition of $Al(BH_4)_3$. This "catalyst" does not affect the Raman spectrum significantly because of its low concentration, but is believed to have a pronounced effect on the NMR spectrum via one of two mechanisms:

1. Catalysis of intramolecular rotation of the BH_4 groups. This might occur by the attack of the "catalyst" on the bridge bonds and the result would be to speed the reorientation, thereby spin-spin decoupling the protons and the Al nucleus. This would eliminate any Al quadrupolar broadening and yield sharp bands as observed.

2. Catalysis of intermolecular exchange of the BH_4 (or BH_3) group. If the "catalyst" provided a ready mechanism for transfer of either a BH_4 or a BH_3 group from one $Al(BH_4)_3$ to another, coupling between the Al and the protons would again be eliminated. Moreover, such an intermolecular exchange process could accommodate Marks and Shimps' mechanism of <u>boron</u> quadrupolar broadening since intermolecular exchange would definitely affect the spin lattice relaxation process. By either mechanism, only trace amounts of "catalyst" need be present and in fact very weak indications of growth of the "catalyst" bands in the Raman spectra of samples kept sealed in capillaries for months at room temperature have been observed. Thus this thesis proposes that there is no such thing

as Type I and II forms of $Al(BH_4)_3$, only varying degrees of contamination due to decomposition products. Although the Type II NMR spectra taken in this thesis indicate that such contamination is present in the liquid samples, the absence of any "catalyst" bands in the liquid and solid Raman spectra ensures the validity of the interpretation of the vibrational spectra in terms of a single $Al(BH_4)_3$ structure.

It is not clear which of the two spin decoupling mechanisms is to be favored nor what the precise nature of the "catalyst" might be although the $Al_2B_4H_{18}$ product proposed by Ogg and Ray would not be unreasonable. Such a complex species would be consistent with the observation of polarized low frequency modes below 400 cm^{-1} and the 795 cm^{-1} band could be the B -- B stretch of the equilibrium partner, B_2H_6. On the other hand, the feature at 2315 cm^{-1} is reminiscent of the BH_4^- symmetric stretch which occurs at 2264, 2255, and 2330 cm^{-1} in $NaBH_4$, CH_3ZnBH_4, and $Be(BH_4)_2$, respectively. In view of the limited information available, however, further work on the liquid phase of $Al(BH_4)_3$ may be in order.

Summary

This work has established that $Al(BH_4)_3$ retains its covalent double hydrogen bridge structure in all three phases and the spectral details can be reasonably interpreted in terms of a D_{3h} prismatic

structure. All of the fundamental vibrations allowed under this symmetry are assigned, and the results provide satisfactory agreement with the Product Rule. A comparison is made with a previous partial assignment and five of the earlier values are changed. Many of the fundamentals fall in characteristic frequency regions, and these assignments should aid in interpreting the spectra of other metal tetrahydroborates. Finally, NMR spectra of liquid $Al(BH_4)_3$ were obtained at various temperatures and some differences from earlier reports were observed. The present results, along with Raman studies of the NMR samples, from -60 to +80°C, are consistent with the existence of a single monomeric form of $Al(BH_4)_3$ over this temperature interval. There is, however, some indication that traces of decomposition products may act as catalysts in BH_4 reorientation or exchange processes which markedly affect the NMR spectra.

Relying in part on some of the results obtained here for $Al(BH_4)_3$ and $Al(BD_4)_3$ the vibrational assignments for C_5H_5BeCl, $C_5H_5BeBH_4$, and $C_5H_5BeBD_4$ are presented in the following chapter. For $C_5H_5BeBH_4$ and $C_5H_5BeBD_4$ these assignments are discussed in terms of the number and orientation (relative to the C_5H_5 ring) of the bridging hydrogens.

IV. CYCLOPENTADIENYLBERYLLIUM TETRAHYDROBORATE

The structural variations observed for $Be(BH_4)_2$ (15, 17) have stimulated interest in other beryllium tetrahydroborates in which one of the tetrahydroborate groups has been replaced by some other ligand. Examples are CH_3BeBH_4 and $C_5H_5BeBH_4$. Gas phase electron diffraction investigations of C_5H_5BeCl (35) and $C_5H_5BeBH_4$ (36) have shown that in both cases the C_5H_5Be fragment has C_{5v} symmetry. However, for $C_5H_5BeBH_4$ these studies were inconclusive as to whether the $BeBH_4$ fragment is doubly or triply hydrogen bridged. In an effort to resolve this question, and to aid in the characterization of the vibrational spectra of other beryllium tetrahydroborate systems, detailed analyses of the infrared and Raman spectra of C_5H_5BeCl, $C_5H_5BeBH_4$, and $C_5H_5BeBD_4$ were undertaken, and the results are presented here with the following additional objectives in mind:

1. To determine whether the molecular structures change significantly in going from the liquid to solid phase.
2. To obtain infrared and Raman spectra of the solid phase to aid in establishing frequencies and to assist in resolving overlapping liquid phase bands.
3. To use this data to separate the C_5H_5 vibrations from the vibrations due to the $BeBH_4$ fragment and to make a complete assignment of all vibrations based on C_{5v} local symmetry for the ring and C_{2v} local symmetry for the tetrahydroborate group.

Results and Discussion

The vibrational spectra of liquid and solid C_5H_5BeCl, $C_5H_5BeBH_4$, and $C_5H_5BeBD_4$ are displayed in Figures 10, 11, and 12 and the corresponding frequencies and assignments listed in Tables 13, 14, and 15, respectively. Comparison of the liquid and solid Raman spectra of $C_5H_5BeBH_4$ and $C_5H_5BeBD_4$ shows only small frequency shifts between the phases and thus it may be concluded that these compounds retain their covalently bonded structures in these phases.

For convenience in interpretation and discussion the assignment of the vibrations in these compounds was broken down as follows:

1. The 24 ring vibrations (4 non-degenerate and 10 doubly degenerate) were assigned under C_{5v} local symmetry and are designated $\nu_{1...14}$.
2. The 12 non-degenerate metal tetrahydroborate fundamental vibrations were assigned under C_{2v} local symmetry and are designated $\nu'_{1...12}$.
3. The remaining 6 skeletal vibrations were assigned under either C_s ($C_5H_5BeBH_4$ and $C_5H_5BeBD_4$) or C_{5v} (C_5H_5BeCl) total symmetries and are designated $\nu''_{1...6}$.

Schematic sketches of these vibrations are listed in Figure 13.

Of the three systems to be studied, only C_5H_5BeCl has sufficient symmetry (C_{5v}) for the infrared and Raman activities to be of

Figure 10. Infrared and Raman spectra of C_5H_5BeCl.

(a) IR spectrum - solid film at 14°K.

(b) Raman spectrum - solid film at 15°K, upper trace 25X lower trace.

(c) Raman spectrum - liquid phase at 50°C, upper trace 25X lower trace.

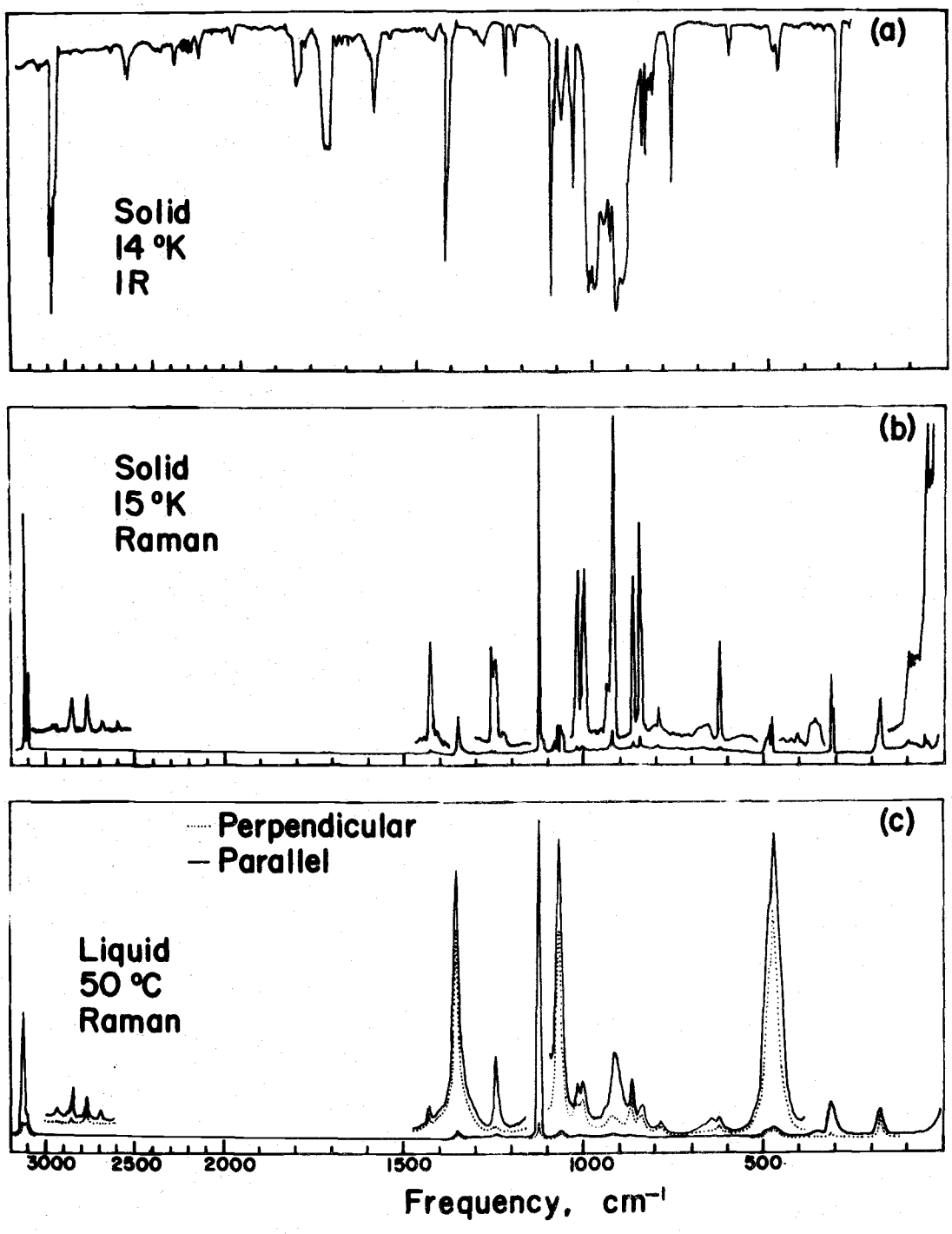
(a)
Solid
14 °K
IR
(b)
Solid
15 °K
Raman
(c)
Perpendicular
Parallel
Liquid
50 °C
Raman
3000
2500
2000
1500
1000
500
Frequency, cm⁻¹

Figure 11. Infrared and Raman spectra of $C_5H_5BeBH_4$.

(a) IR spectrum - solid film at 14°K.

(b) Raman spectrum - solid film at 14°K, upper trace 10X lower trace.

(c) Raman spectrum - liquid phase at 25°C, upper trace 20X lower trace.

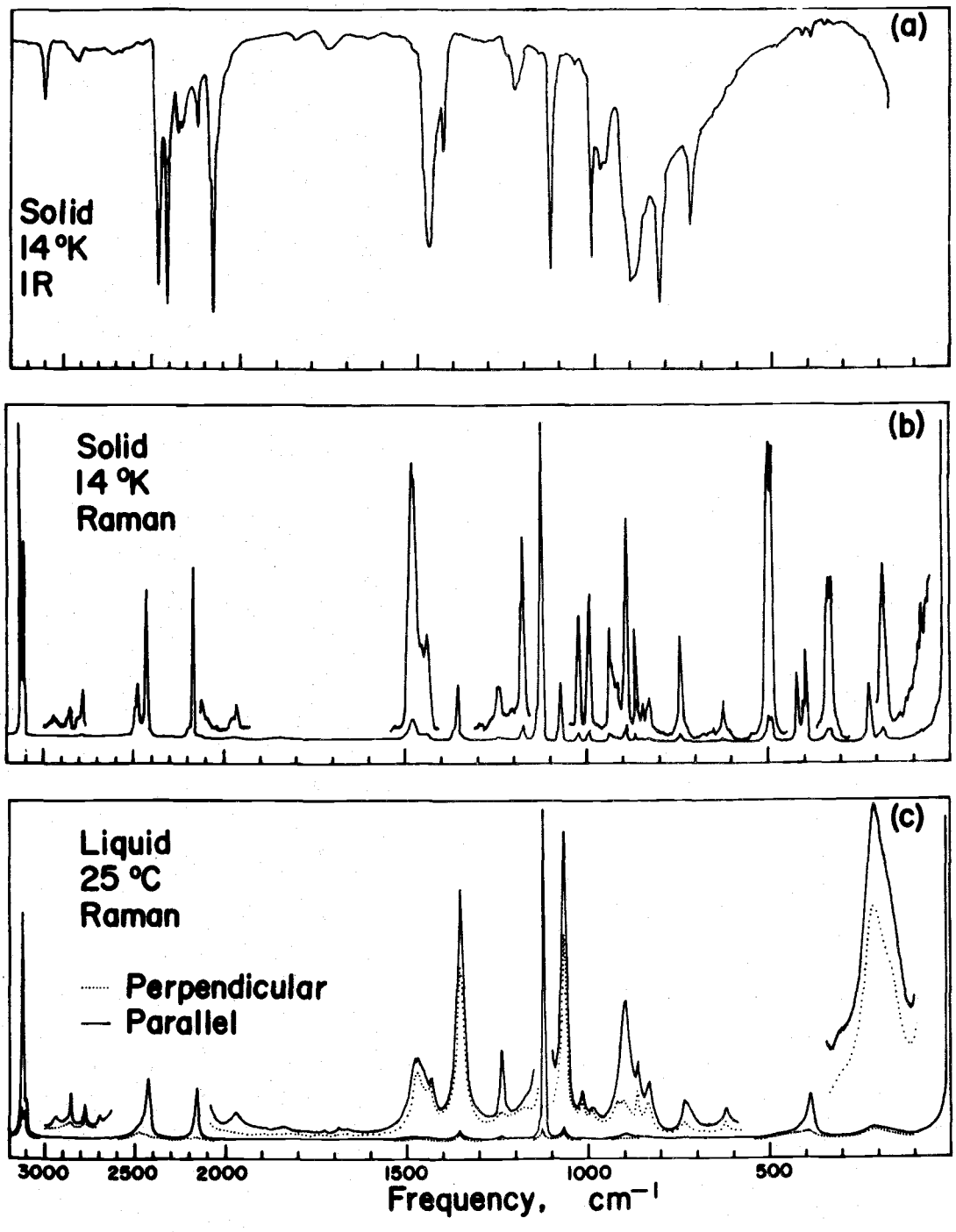
(a)
Solid
14 °K
IR
(b)
Solid
14 °K
Raman
(c)
Liquid
25 °C
Raman
Perpendicular
Parallel
3000
2500
2000
1500
1000
500
Frequency, cm⁻¹

Figure 12. Infrared and Raman spectra of $C_5H_5BeBD_4$.

(a) IR spectrum - solid film at 14°K.

(b) Raman spectrum - solid film at 15°K, upper trace 7.5 X lower trace.

(c) Raman spectrum - liquid phase at 25°C, upper trace 50X lower trace.

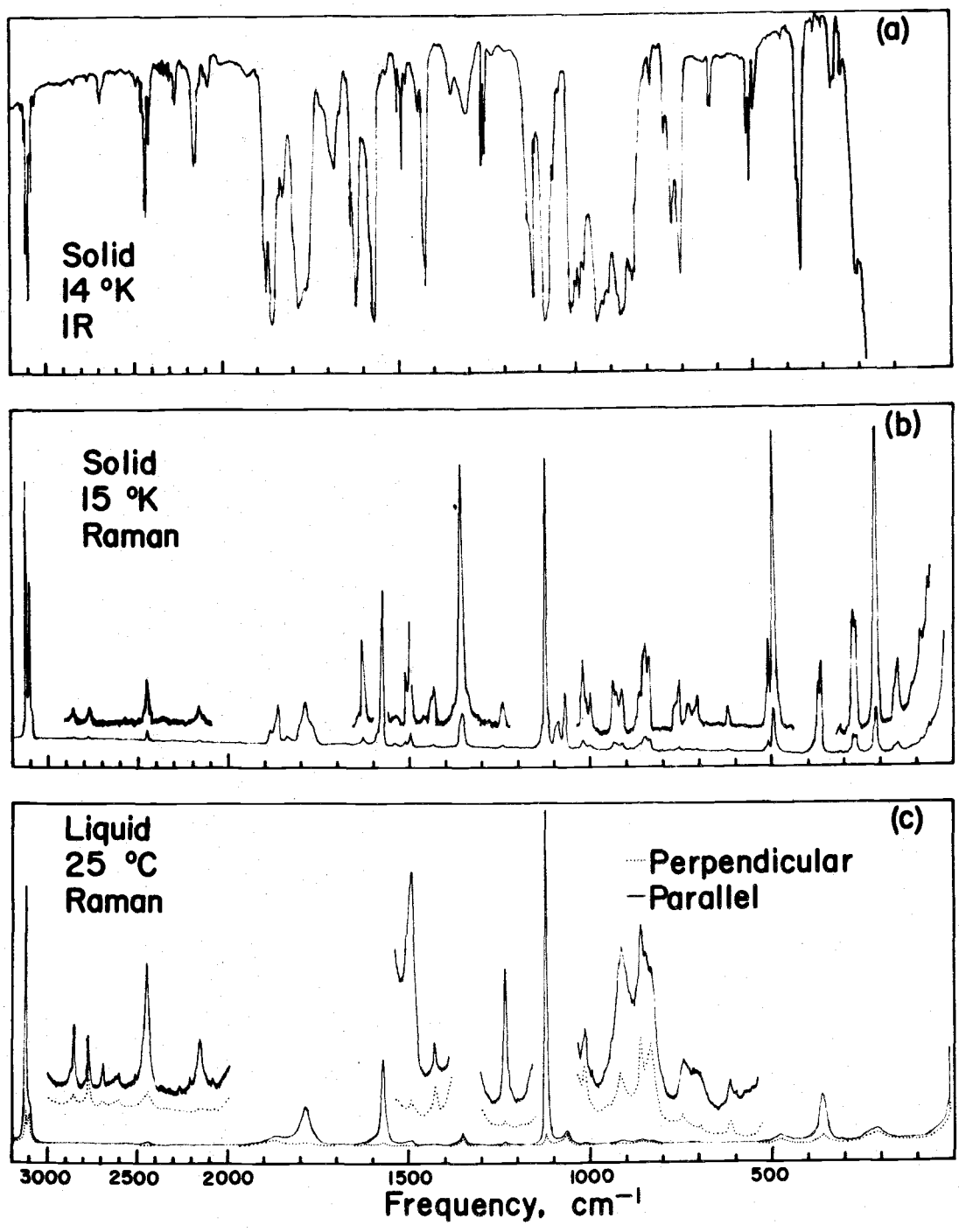
(a)
Solid
14 °K
IR
(b)
Solid
15 °K
Raman
(c)
Liquid
25 °C
Raman
Perpendicular
Parallel
3000
2500
2000
1500
1000
500
Frequency, cm⁻¹

Table 13. Vibrational frequencies (cm^{-1}) of C_5H_5BeCl.

IR Solid 14°K	Raman Solid 14°K	Raman Liquid 50°C	ρ	C_{5v}	Assignment	
3120 s	3120 vs	3124 vs	0.13	A_1	ν_1	
3112 vs	3112 s			E_1	ν_5	
	3103 vs	3104 s,sh	0.6	E_2	ν_9	
2852 vw	2850 vw	2853 w	0.22	A_1	$2\nu_6$	= 2854
2771 vw	2770 vw	2774 w	0.82	E_1	$\nu_6 + \nu_{10}$	= 2779
2694 w		2692 vw	0.17	A_1	$2\nu_{10}$	= 2704
2409 w				E_1	$\nu_{10} + \nu_{12}$	= 2418
2275 w				E_1	$\nu_6 + \nu_8$	= 2292
2081 w				E_1	$\nu_{11} + \nu_{13}$	= 2096
1851 m				E_1	$\nu_7 + \nu_{13}$	= 1858
1764 s				E_1	$\nu_5' + \nu_8$	= 1785
1628 s				E_1	$\nu_7 + \nu_{14}$	= 1635
1489 w				E_1	$\nu_8 + \nu_{14}$	= 1490

Table 13. Vibrational frequencies (cm^{-1}) of C_5H_5BeCl. (Continued)

IR Solid 14°K	Raman Solid 14°K	Raman Liquid 50°C	ρ	C_{5v}	Assignment	
1459 vw				E_1	$\nu_{13} + \nu_{14}$	= 1473
1427 vs	1427 m	1430 w	0.7	E_1	ν_6	
	1352 s	1352 s	0.82	E_2	ν_{10}	
1327 w				E_1	$\nu''_{3,2} + \nu_{13}$	= 1330
1256 m	1259 m					
1249 vw	1248 m	1244 m	0.08	E_2,A_1	$\nu_{11},2\nu_{14}$	= 1250
1233 w	1232 vw			A_1	$\nu'_5 + \nu''_1$	= 1234
1126 vs	1125 vs	1126 vs	0.04	A_1	ν_2	
1118 w,sh	1119 s	1120 w,sh	0.1	A_1	ν_2 (C^{13})	
1100 s	1102 m			E_1	$\nu'_5 + \nu''_{5,4}$	= 1096
1074 s	1073 s					
	1066 s	1066 s	0.81	E_2	ν_{12}	
1064 s	1063 m					
1019 vs	1018 m	1017 w	0.79	E_1	ν_7	

Table 13. Vibrational frequencies (cm^{-1}) of C_5H_5BeCl. (Continued)

IR Solid 14°K	Raman Solid 14°K	Raman Liquid 50°C	ρ	C_{5v}	Assignment	
1013 w						
1000 vs	1002 m	1000 w	0.75	E_1	$\nu''_{5,4} + \nu_{13}$	= 1014
974 m				E_1	$\nu_3 + \nu''_{5,4}$	= 962
956 m				E_1	$2\nu''_{3,2}$	= 964
939 vs	940 w					
919 vs	920 s	912 m	0.23	A_1	ν'_5	
865 s	866 m	865 w	0.69	E_1	ν_8	
855 s						
846 vw	848 m					
838 w	842 w,sh	837 w	0.72	E_2	ν_{13}	
786 s	794 vw	785 vw	0.63	A_1	ν_3	
		646 vw	0.3	A_1	$\nu''_{3,2} + \nu''_{5,4}$	= 658
623 w	625 m	624 vw	0.54	E_2, A_1	$\nu_{14}, 2\nu''_1$	= 628
496 vw	493 m,sh			E_1	$\nu''_1 + \nu''_{5,4}$	= 500

Table 13. Vibrational frequencies (cm^{-1}) of C_5H_5BeCl. (Continued)

IR Solid 14°K	Raman Solid 14°K	Raman Liquid 50°C	ρ	C_{5v}	Assignment	
	485 s	486 m,sh	0.7	E_1	$\nu''_1 + \nu''_{5,4}$	= 489
482 m	479 s	474 s	0.80	E_1	ν''_3, ν''_2	
	357 vw,b	347 w,sh	0.1	A_1	$2\nu''_{5,4}$	= 352
314 s	314 s	312 vs	0.12	A_1	ν''_1	
309 w,sh	310 m,sh				ν''_1 (Cl^{37})	
	186 m,sh					
	175[a] s	177 vs	0.78	E_1	ν''_5, ν''_4	

[a] Raman active lattice modes were also observed at 101 m, 93 m, 81 m, 50 m, and 41 m cm^{-1}.

Table 14. Vibrational Frequencies (cm^{-1}) of $C_5H_5BeBH_4$.

IR Solid 14°K	Raman Solid 14°K	Raman Liquid 50°C	ρ	C_s[a] C_{5v}	C_{2v}	Assignment	
3125 w	3123 vvs	3123 vvs	0.12	A_1		ν_1	
3118 m							
3110 m				E_1		ν_5	
3102 w	3103 vs	3104 vs	0.8	E_2		ν_9	
2938 w	2930 vvw	2938 vvw	0.00		A_1	$2\nu'_{11}$	= 2940
	2855 vw	2858 vw	0.16	A_1		$2\nu_6$	= 2870
	2777 vw	2778 vw	0.80	E_2		$\nu_6 + \nu_{10}$	= 2788
	2696 vvw	2694 vvw	0.10	A_1		$2\nu_{10}$	= 2706
2477 vs	2473 s	2479 s	0.6		B_1	ν'_7	
2426 vs	2422 vs	2428 vs	0.06		A_1	ν'_1	
2251 w	2252 vw			A_1		$2\nu_2$	= 2246
2170 vs					B_2	ν'_{10}	
	2166 vs	2162 vs	0.05		A_1	ν'_2	

Table 14. Vibrational frequencies (cm^{-1}) of $C_5H_5BeBH_4$. (Continued)

IR Solid 14°K	Raman Solid 14°K	Raman Liquid 50°C	ρ	C_s[a] C_{5v}	C_{2v}	Assignment	
	1964 vw	1969 vw	0.12	A_1		$\nu_3 + \nu_{11}$	= 1974
1750 w,b				A'+A"		$\nu_8+\nu_5'$	= 1751
		1685 vvw	0.19	A_1		$2\nu_{13}$	= 1686
1477 vs	1478 m				A_1	ν_3'	
1470 vs	1472 m	1476 w	0.76		B_2	ν_{11}'	
1434 m	1435 w	1433 vw	0.8	E_1		ν_6	
	1353 s	1355 s	0.83	E_2		ν_{10}	
1262 vw				A'		$\nu_5' + \nu_1''$	= 1280
1235 vw	1239 w	1238 w	0.06	E_2,A_1+E_1		ν_{11},$2\nu_{14}$	= 1244
	1173 m	1176 vvw,sh	dP,?		A_2	ν_6'	
1131 vs	1131 vvw				A_1	ν_4'	
1124 s,sh	1123 vvs	1124 vvs	0.05	A_1		ν_2	
	1070 s	1067 s	0.76	E_2		ν_{12}	
1065 vw				A'+A"		$\nu_{3,2}'' + \nu_{12}'$	= 1063

Table 14. Vibrational frequencies (cm^{-1}) of $C_5H_5BeBH_4$. (Continued)

IR Solid 14°K	Raman Solid 14°K	Raman Liquid 50°C	ρ	C_{5v}	C_s [a]	C_{2v}	Assignment	
1016 vs	1019 m	1016 vw	0.72	E_1			ν_7	
	996 vw,sh				A''		$\nu''_6 + \nu'_{12}$	= 1006
990 m	990 m	990 vvw	0.6			B_1	ν'_8	
973 m,sh					A'		$2\,''_{3,2}$	= 985
935 m,sh	936 w				A'		$2\,''_{3,2}$	= 976
921 m,sh	921 vw,sh	920 vw,sh	dp,?		A''+A'		$\nu''_{5,4} + \nu_3$	= 957
904 vs	913 vw	906 vw	dp,?		A''		$\nu''_6 + \nu_3$	= 919
889 vs	888 m	896 m	0.15		A'		ν'_5	
863 vw,sh	863 m	864 w	0.72	E_1			ν_8	
	843 vw	834 w	0.65	E_2			ν_{13}	
823 vs	824 vw					B_2	ν'_{12}	
735 s	739 m	735 w	0.34	A_1			ν_3	
	622 w	619 vw	0.54	E_2			ν_{14}	
	497 m				A'',A'		ν''_3,ν''_2	

Table 14. Vibrational frequencies (cm^{-1}) of $C_5H_5BeBH_4$. (Continued)

IR Solid 14°K	Raman Solid 14°K	Raman Liquid 50°C	ρ	C_s[a] C_{5v}	C_{2v}	Assignment	
486 vw	488 m	471 m,sh	dp,?	A",A'		ν''_3,ν''_2	
416 vw	418 s	418 m,sh	dp,?	A'		$2\nu''_{5,4}$	= 440
	401 m			A'+A"		$\nu''_6 + \nu''_{4,5}$	= 402
391 vw	392 s	389 vs	0.14	A'		ν''_1	
	332 m				B_1	ν'_9	
	324 m	314 vw,sh	dp,?				
	220 s	213 s	0.79	A",A'		ν''_5,ν''_4	
	182[b] m	171 m,sh	.8	A"		ν''_6	

[a] C_s is the total molecular symmetry. C_{5v} and C_{2v} are local symmetries for the C_5H_5 and metal tetrahydroborate groups, respectively.

[b] Raman active lattice modes were also observed at 117 w, 84 vw, and 76 w cm^{-1}.

Table 15. Vibrational frequencies (cm^{-1}) of $C_5H_5BeBD_4$.

IR Solid 14°K	Raman Solid 14°K	Raman Liquid 50°C	ρ	C_s[a] C_{5v}	C_{2v}	Assignment	
3123 vw	3121 vvs	3124 vvs	0.11	A_1		ν_1	
3117 s							
3111 s				E_1		ν_5	
3107 s							
3102 m,sh	3102 vs	3105 vs	0.6	E_2		ν_9	
3093 m	3093 m,sh						
	2854 vw	2856 w	0.24	A_1		$2\nu_6$	= 2860
	2775 vw	2776 w	0.76	E_1+E_2		$\nu_6 + \nu_{10}$	= 2782
2701 w		2696 vw	0.20	A_1		$\nu_2 + \nu_2'$	= 2698
2496 vw				E_1+E_2		$\nu_6 + \nu_{12}$	= 2499
2470 vw	2470 vvw				B_1	ν_{BH_t}, BH_2D_2	
2446 m	2447 w	2453 m	0.11		A_1	ν_{BH_t}, BHD_3	
2427 w	2427 vvw				A_1	ν_{BH_t}, BH_2D_2	
2273 w		2270 vvw	0.34		A_1	$\nu_2' + \nu_{12}'$	= 2278

Table 15. Vibrational frequencies (cm^{-1}) of $C_5H_5BeBD_4$. (Continued)

IR Solid 14°K	Raman Solid 14°K	Raman Liquid 50°C	ρ	C_s[a] C_{5v}	C_{2v}	Assignment	
		2215 vvw	0.12	A_1		$\nu_8 + \nu_{10}$	= 2214
2167 m	2164 vw	2158 w	0.12		A_1	ν_{BH_b}, BHD_3	
2089 vw		2087 vvw	0.68	A' + A"		$\nu'_5 + \nu_{11}$	= 2087
1882 s	1882 w,sh			$A_1+A_2+E_2$		$\nu_7 + \nu_8$	= 1880
1864 vs	1864 s	1869 s	dp,?		B_1	ν'_7	
1833 w	1835 vw				A_1	ν_{BD_t}, BHD_3	
1789 vs	1789 s	1786 vs	0.07		A_1	ν'_1	
1767 m,sh	~1765 s			A'+A"		$\nu'_{12} + \nu_{12}$	= 1773
1690 m				A'		$2\nu'_5$	= 1694
1640 m,sh					B_2	$\nu'_4 + \nu'_{12}$	= 1641
1627 vs	1627 w	1623 w	0.4		B_2	ν'_{10}	
1575 vs	1573 vs	1573 vs	0.06		A_1	ν'_2	
1508 w	1508 w			A'+A"		$\nu_7 + \nu''_{3,2}$	= 1515
1495 m	1495 m	1494 s	0.04		A_1	$2\nu'_8$	= 1503

Table 15. Vibrational frequencies (cm^{-1}) of $C_5H_5BeBD_4$. (Continued)

IR Solid 14°K	Raman Solid 14°K	Raman Liquid 50°C	ρ	C_{5v}	C_s[a] C_{2v}	Assignment	
1449 vw					A'	$\nu''_1 + \nu'_3$	= 1453
1430 s	1431 w	1432 vw	0.76	E_1		ν_6	
1353 w	1352 s	1354 s	0.86	E_2		ν_{10}	
1306 w					A''+A'	$\nu''_{5,4} + \nu'_{11}$	
1265 m							
1261 m					A'+A''	$\nu_7 + \nu'_9$	= 1290
1257 w							
1242 vvw	1240 w	1239 m	0.07	E_2,A_1+E_1		ν_{11}, $2\nu_{14}$	= 1240
1137 m,sh					A'+A''	$\nu''_{3,2} + \nu_{14}$	
1125 s	1124 vvs	1125 vvs	0.03	A_1		ν_2	
1092 vs					B_2	ν'_{11}	
1086 vs	1087 m				A_1	ν'_3	
1067 w,sh	1069 s	1068 s	0.86	E_2		ν_{12}	
1017 vs	1019 m	1019 w	0.83	E_1		ν_7	

Table 15. Vibrational frequencies (cm^{-1}) of $C_5H_5BeBD_4$. (Continued)

IR Solid 14°K	Raman Solid 14°K	Raman Liquid 50°C	ρ	C_{5v}	C_s [a]	C_{2v}	Assignment	
1000 w,sh	999 w				A'		$2\nu''_{3,2}$	= 1006
989 s					A'		$2\nu''_{3,2}$	= 994
979 w,sh					A''		$\nu'_9 + \nu'_{12}$	= 980
941 vs	935 w	918 m	0.23			A_1	ν'_4	
921 w,sh					A''+A'		$\nu''_{5,4} + \nu_3$	= 942
908 s,sh	913 w				A'' +A'		$\nu''_{5,4} + \nu'_{12}$	= 917
868 vs	862 vw	863 m	0.6	E_1			ν_8	
849 w,sh	847 m	852 w,sh	0.4		A'		ν'_5	
840 s					A''		$\nu''_6 + \nu'_{12}$	= 856
834 w,sh	836 m,sh	836 m,sh	0.7	E_2		A_2	ν_{13}, ν'_6	
787 w					A'+A''		$\nu'_9 + \nu''_{3,2}$	= 782
749 w,sh	754 w	750 w	0.3			B_1	ν'_8	
729 m,sh	729 vw	735 w,sh	0.2	A_1			ν_3	
704 s	704 vw	708 w,sh	0.1			B_2	ν'_{12}	

Table 15. Vibrational frequencies (cm^{-1}) of $C_5H_5BeBD_4$. (Continued)

IR Solid 14°K	Raman Solid 14°K	Raman Liquid 50°C	ρ	C_{5v}	C_s[a] C_{2v}	Assignment	
624 w					B_1	$\nu''_1 + \nu'_9$	= 634
618 w	620 w	619 vw	0.87	E_2		ν_{14}	
515 w,sh	515 vw,sh				A'	$\nu''_1 + \nu''_6$	= 518
509 m	509 m,sh				A',A''	ν''_3, ν''_2	
496 w	497 s	482 s	0.77		A',A''	ν''_3, ν''_2	
419 vvw					A'	$2\nu''_{5,4}$	= 426
373 w,sh	374 s				A'+A''	$\nu''_6 + \nu''_{5,4}$	= 365
366 s	366 vs	365 vs	0.18		A_1	ν''_1	
278 w	274 m						
269 w	268 m,sh				B_1	ν'_9	
210 m	213 s	216 s	0.84		A',A''	ν''_5, ν''_4	
	152[b] m				A''	ν''_6	
		122 vvw	0.40		A'	$\nu'_9 - \nu''_6$	

Table 15. Vibrational frequencies (cm^{-1}) of $C_5H_5BeBD_4$. (Continued)

---

[a] C_s is the total molecular symmetry. C_{5v} and C_{2v} are local symmetries for the ring and metal tetrahydroborate groups, respectively.

[b] Raman active lattice modes were also observed at 87 vw and 68 vw cm^{-1}.

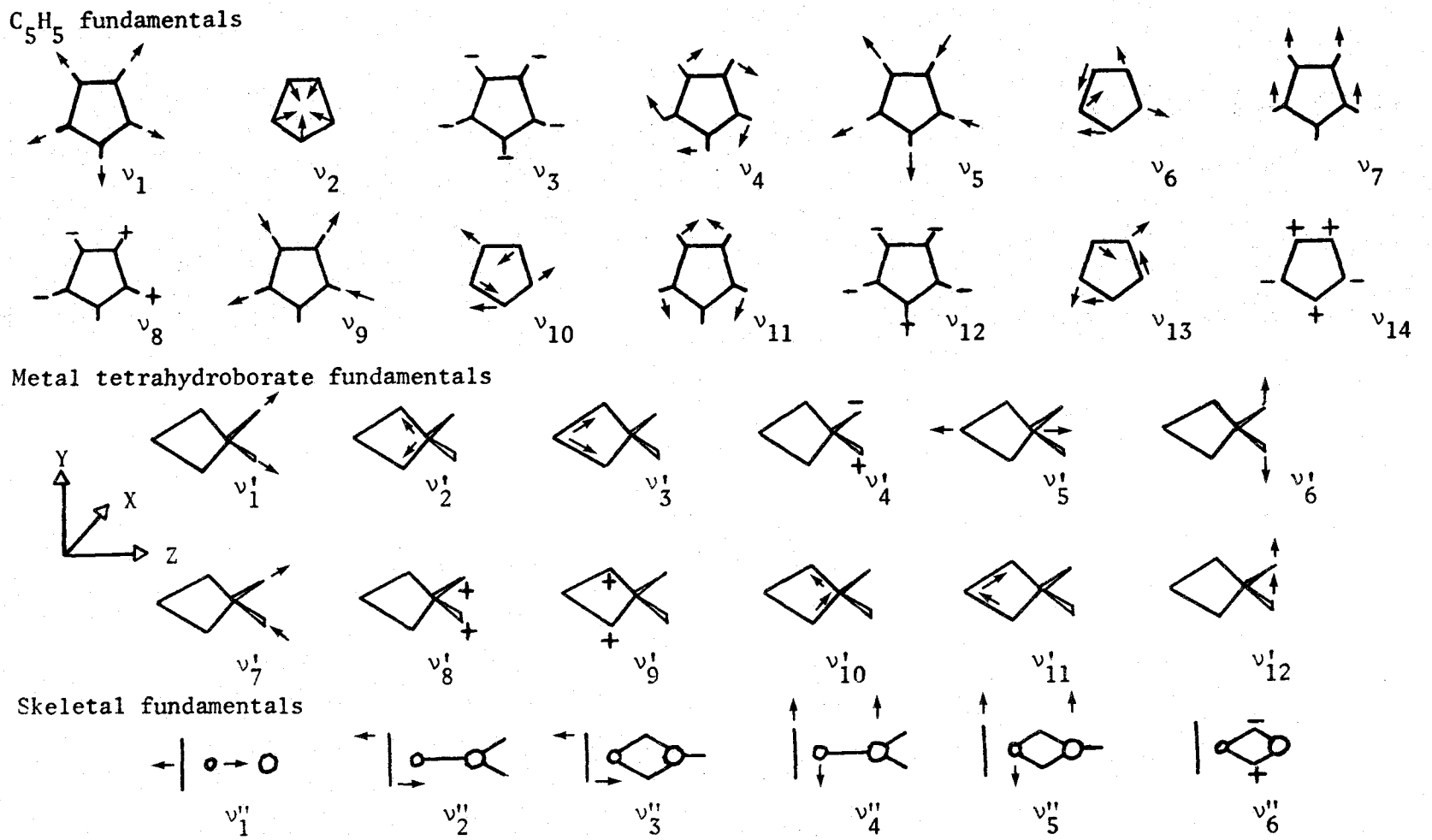

Figure 13. Schematic sketches of the C_5H_5 ring, metal tetrahydroborate, and skeletal fundamental vibrations.

much help in assigning the vibrations, hence the assignments must rely heavily on previous work on similar systems. To this end the C_5H_5 ring fundamentals of $(C_5H_5)_2Fe$ (37) and $C_5H_5^-K^+$ (38) have been listed in Table 16 along with the assignments for C_5H_5BeCl, $C_5H_5BeBH_4$, and $C_5H_5BeBD_4$. Table 17 lists the fundamental assignments and frequencies for the $BeBH_4$ and $BeBD_4$ molecular fragments and compares them to the corresponding values for $BeBH_4^+$ and $BeBD_4^+$ (15). Finally, Table 18 presents the assignments for the skeletal vibrations of C_5H_5BeCl, $C_5H_5BeBH_4$, and $C_5H_5BeBD_4$ and compares them with the skeletal modes of $(C_5H_5)_2Fe$ (37).

The frequency values given in these tables are, where possible, taken from the infrared and Raman spectra of the solid phase.

Crystal splittings were observed for a number of features in the solid spectra and in these instances an average value for the observed frequencies is listed in Tables 16, 17, and 18.

C_5H_5 Ring Vibrations

In assigning the C_5H_5 vibrations in C_5H_5BeCl, $C_5H_5BeBH_4$, and $C_5H_5BeBD_4$, the analysis for C_5H_5BeCl played a key role for two reasons. First, the spectra of C_5H_5BeCl should be relatively uncluttered, since in addition to the C_5H_5 vibrations there are only six low frequency skeletal modes. Second, the infrared and Raman studies of C_5H_5BeCl provide enough information to distinguish between those

Table 16. C_5H_5 Fundamental Frequencies (cm^{-1}).

	Mode	D_{5h}		C_{5v}		C_5H_5BeCl	$C_5H_5BeBH_4$	$C_5H_5BeBD_4$	$(C_5H_5)_2Fe$(37)	$C_5H_5^-K^+$(38)
ν_1	ν_{CH}	A_1'	R	A_1	IR,R	3120	3123	3121	3110,3103	3043
ν_2	ν_{CC}	A_1'	R	A_1	IR,R	1126	1124	1124	1102,1110	983
ν_3	δ_{CH} out of plane	A_2''	IR	A_1	IR,R	790	737	729	814,820	710
ν_4	δ_{CH} in plane	A_2'	--	A_2	--	--	--	--	(1250,1255)	--
ν_5	ν_{CH}	E_1'	IR	E_1	IR,R	3112	3114	3114	3086,3077	3039
ν_6	ν_{CC}	E_1'	IR	E_1	IR,R	1427	1435	1430	1410,1410	1455
ν_7	δ_{CH} in plane	E_1'	IR	E_1	IR,R	1018	1017	1018	1005,998	1003
ν_8	δ_{CH} out of plane	E_1''	R	E_1	IR,R	866	863	862	855,844	625
ν_9	ν_{CH}	E_2'	R	E_2	R	3103	3103	3102	3100,3085	3096
ν_{10}	ν_{CC}	E_2'	R	E_2	R	1352	1352	1352	1356,1351	1447
ν_{11}	δ_{CH} in plane	E_2'	--	E_2	R	(1248)	(1239)	(1241)	1205,1188	1020
ν_{12}	δ_{CH} out of plane	E_2''	--	E_2	R	1066	1070	1069	1058,1055	--
ν_{13}	δ_{ring} in plane	E_2'	R	E_2	R	848	834	846	897,885	565
ν_{14}	δ_{ring} out of plane	E_2''	--	E_2	R	625	622	620	597,569	--

Table 17. $BeBH_4$ and $BeBD_4$ fundamental frequencies (cm^{-1}).

	Mode		C_{2v}		$C_5H_5BeBH_4$	$C_5H_5BeBD_4$	H/D	$BeBH_4^+$	$BeBD_4^+$	H/D
ν_1'	ν_{BH_t}	sym	A_1	IR,R	2424	1789	1.35	2450	1802	1.36
ν_2'	ν_{BH_b}	sym	A_1	IR,R	2166	1574	1.38	2118	1502	1.41
ν_3'	ν_{BeH_b}	sym	A_1	IR,R	1475	1087	1.36	1540	1077	1.43
ν_4'	$\delta_{BH_{2t}}$	deformation	A_1	IR,R	1131	938	1.21	1128	823	1.37
ν_5'	ν^a_{BeB}	asym	A_1	IR,R	888	847	1.05	722	700	1.04
ν_6'	$\delta_{BH_{2t}}$	torsion	A_2	R	1173	(836)	1.40	--	--	--
ν_7'	ν_{BH_t}	asym	B_1	IR,R	2475	1864	1.33	2510	1892	1.32
ν_8'	$\delta_{BH_{2t}}$	rock	B_1	IR,R	990	750	1.32	1010[b]	791	1.27
ν_9'	δ_{BeH_2B}	bridge bend	B_1	IR,R	328	271	1.21	405	346	1.17
ν_{10}'	ν_{BH_b}	asym	B_2	IR,R	2170	1627	1.33	2075	1557	1.33
ν_{11}'	ν_{BeH_b}	asym	B_2	IR,R	1470	1092	1.35	(1540)[c]	(1077)[c]	1.43
ν_{12}'	$\delta_{BH_{2t}}$	wag	B_2	IR,R	823	704	1.17	970[b]	834	1.16

[a] ν_{BeCl} (C_5H_5BeCl) = 920 cm^{-1}.

Table 17. $BeBH_4$ and $BeBD_4$ fundamental frequencies (cm^{-1}). (Continued)

[b] The assignments given in reference 15 for ν_8' and ν_{12}' have been reversed in this table to be more consistent with these recent results on $Al(BH_4)_3$ and $C_5H_5BeBH_4$.

[c] The assignment of ν_{11}' for $BeBH_4^+$ has been changed from values of 1430 (1023) cm^{-1} (15) because recent work on CH_3Zn^+ BH_4^- (17) has suggested that the latter bands are due to BH_4^-.

Table 18. Skeletal Frequencies (cm^{-1}).

	Mode	C_{5v}		C_s		C_5H_5BeCl	$C_5H_5BeBH_4$	$C_5H_5BeBD_4$	H/D	$(C_5H_5)_2Fe$
ν''_1	ν_{CpBe} sym	A_1	IR,R	A'	IR,R	314	392	366	1.07	478
ν''_2, ν''_3	δ ring tilt	E_1	IR,R	A'+A"	IR,R	482	497,488	509,497	0.98	492,389
ν''_4, ν''_5	δ_{CpBeX}[a]	E_1	IR,R	A'+A"	IR,R	176	220	214	1.03	179
ν''_6	δ torsion	--		A"	IR,R	--	182	152	1.20	130[b]

[a] X = Cl, BH_4, BD_4.

[b] $(C_5H_5)_2Ru$ (37).

vibrations corresponding to different C_{5v} symmetry species (the A_1 vibrations will be polarized in Raman studies of the liquid phase, the E_1 vibrations will have coincident infrared and Raman frequencies, and the E_2 vibrations will be Raman active only). Additional information concerning the expected activities and intensities of the C_5H_5 vibrations can be obtained by assuming local D_{5h} symmetry for the C_5H_5 ring. To this end the symmetries and activities of the C_5H_5 vibrations under D_{5h} symmetry have been included in Table 16. Furthermore, for $C_5H_5BeBH_4$ and $C_5H_5BeBD_4$ those bands which do not shift upon deuteration of the tetrahydroborate group can be assumed to be associated with vibrational motions of the C_5H_5 ring. That bands in $C_5H_5BeBH_4$ and $C_5H_5BeBD_4$ could be assigned as C_5H_5 modes and show agreement within ± 8 cm^{-1} (see Table 16) is support for the above statement and is indicative of little vibrational coupling between the tetrahydroborate group and the C_5H_5 ring.

The frequencies of the fundamental vibrations of the cyclopentadienyl group in sandwich compounds are quite characteristic, varying only slightly from compound to compound (38). The in-phase and out-of-phase frequencies associated with the two rings in these sandwich compounds are very nearly the same (see the $(C_5H_5)_2Fe$ frequencies listed in Table 16). This suggests that there is very little coupling between the rings and that replacement of one of the C_5H_5 rings with Cl, BH_4, or BD_4 will shift the frequencies of the remaining ring only slightly. Comparison of the C_5H_5BeCl spectra with

recent assignments for crystalline $(C_5H_5)_2Fe$ (37) and $C_5H_5^-K^+$ (38), along with consideration of the vibrational activities for C_5H_5BeCl under C_{5v} (total) and D_{5h} (local) symmetries allowed the C_5H_5 vibrations in C_5H_5BeCl to be assigned. The assignments for C_5H_5BeCl, $C_5H_5^-K^+$, and $(C_5H_5)_2Fe$ were then used along with isotopic shift data for $C_5H_5BeBH_4$ and $C_5H_5BeBD_4$ in assigning the C_5H_5 vibrations in these latter two compounds.

The following discussion of the C_5H_5 group is divided into sections describing the vibrations of localized portions of the C_5H_5 ring. The values of the frequencies cited are taken from Table 16 and listed in the order C_5H_5BeCl, $C_5H_5BeBH_4$, $C_5H_5BeBD_4$. For convenience, the number and symmetry of each mode will be given in terms of C_{5v} symmetry, a model which holds strictly for C_5H_5BeCl but only approximately for $C_5H_5BeBH_4$ and $C_5H_5BeBD_4$.

CH Stretches

In the CH stretching region, which is widely separated from any other absorptions, three normal modes are expected. These modes and their activities are:

	D_{5h}		C_{5v}	
ν_1	A_1'	R(P)	A_1	IR,R(P)
ν_5	E_1'	IR	E_1	IR,R
ν_9	E_2'	R	E_2	R

The strong Raman band at 3120, 3123, 3121 cm^{-1}, which is polarized in the Raman spectra of the liquid, is easily identified as ν_1. ν_9 is assigned as the strong 3103, 3103, 3102 cm^{-1} Raman band, since no IR active counterpart was observed for C_5H_5BeCl, where C_{5v} symmetry holds rigidly. The remaining IR and R active band at 3112, 3114, 3114 cm^{-1} is assigned as ν_5. It may be noted that the degenerate modes, ν_5 and ν_9, were split slightly by crystal interactions for solid $C_5H_5BeBH_4$ and $C_5H_5BeBD_4$.

CH Bends

Discussion of the CH bends will be in terms of in plane and out of plane motions. There is some justification in this division in that other studies of C_nH_n ring systems (39,40) have shown that, in general, the in plane CH bends occur at higher frequencies than the out of plane CH bends.

Three CH in plane bending modes are expected. These modes, their activities, and their assignments in $(C_5H_5)_2Fe$ (37) are:

		D_{5h}		C_{5v}		$(C_5H_5)_2Fe$
ν_4	A_2'	--		A_2	--	(1250,1255)
ν_7	E_1'	R		E_1	IR,R	1005,998
ν_{11}	E_2'	R		E_2	R	1205,1188

Of these in plane bends ν_4, inactive for C_5H_5BeCl, was not observed in either $C_5H_5BeBH_4$ or $C_5H_5BeBD_4$ where under C_s symmetry it is active.

Since for the local ring symmetries, C_{5v} and D_{5h}, ν_4 is inactive, the failure to observe it in $C_5H_5BeBH_4$ and $C_5H_5BeBD_4$ is further support for the use of local symmetries in describing the vibrations of the ring. The strongly infrared active, moderately Raman active band observed at 1018 cm^{-1} in the Raman spectrum of solid C_5H_5BeCl was attributed to ν_7. This mode appears at 1017 cm^{-1} and 1018 cm^{-1} in the Raman spectra of $C_5H_5BeBH_4$ and $C_5H_5BeBD_4$, respectively. An alternative assignment of ν_7 at 1001, 990, 989 was considered but rejected on the basis of intensities and because these frequencies were more easily accounted for as combination bands than were the 1018, 1017, and 1018 features.

For all three compounds the Raman spectra of the liquid phase show only a single strongly polarized mode at 1244, 1238, 1239 cm^{-1} in the 1150 cm^{-1} to 1300 cm^{-1} region in which ν_{11} is expected to occur. In solid C_5H_5BeCl this band is observed to split into two coincident infrared (1249 cm^{-1} and 1256 cm^{-1}) and Raman (1248 cm^{-1} and 1259 cm^{-1}) features, one of which could conceivably be ν_{11}. Similarly, a number of features are observed in the infrared spectra of solid $C_5H_5BeBH_4$ (1262 cm^{-1} and 1235 cm^{-1}) and $C_5H_5BeBD_4$ (1265, 1261, 1257, and 1242 cm^{-1}). Most of these can be reasonably explained as overtone or combination bands and in fact the polarized behavior of the 1244, 1238, 1239 cm^{-1} feature may be attributed to $2\nu_{14}$ = 1250, 1244, 1242 cm^{-1}. A careful search from 900 cm^{-1} to 1300 cm^{-1} yielded no plausible alternatives for ν_{11} and thus the 1248, 1239, 1241 cm^{-1} feature (ob-

served to be less intense in the infrared than the other possibilities) is tentatively assigned as this mode.

The activities and assignments in $(C_5H_5)_2Fe$ (37) of the three CH out of plane vibrations are:

	D_{5h}		C_{5v}		$(C_5H_5)_2Fe$
ν_3	A_2''	IR	A_1	IR,R	814,820
ν_8	E_1''	R	E_1	IR,R	855,844
ν_{12}	E_2''	--	E_2	R	1085,1055

Because of its Raman inactivity for D_{5h} symmetry, the symmetric out of plane CH bend, ν_3, is expected to be more intense in the infrared than in the Raman. On this basis the strongly infrared active, weak polarized Raman feature at 790, 737, 729 cm^{-1} is favored over the other polarized band in this region (920, 888, 847 cm^{-1}) as the choice for ν_3. The significant isotopic shift observed for this latter band suggests some involvement of tetrahydroborate motion in this vibration, hence it will later be assigned as ν_5', the ring - beryllium stretch.

ν_{12} is infrared inactive in C_5H_5BeCl and would be expected to be only weakly infrared active for $C_5H_5BeBH_4$ and $C_5H_5BeBD_4$. Thus the strong Raman bands at 1066, 1070, 1069 cm^{-1} are assigned as ν_{12}. The other possibilities for ν_{12} at 1074 cm^{-1} and 1063 cm^{-1} in C_5H_5BeCl are rejected on the basis of their infrared activity. Assignments for these and several other features not believed to be fundamentals will be discussed later.

The remaining CH out of plane bend, ν_8, is assigned as the coincident infrared and Raman band at 866, 863, 862 cm^{-1}. The other possible choice for ν_8 in this region is the band at 848, 843, 846 cm^{-1}. However, no infrared counterpart of this band could be found for $C_5H_5BeBH_4$, and for this and other reasons discussed later this band is assigned as the in plane ring bend, ν_{13}.

CC Motions

The symmetries, activities, and assignments in $(C_5H_5)_2Fe$ (37) for the five fundamental vibrations of the CC framework are:

	D_{5h}		C_{5v}		$(C_5H_5)_2Fe$ (cm^{-1})
ν_2	A_1'	R	A_1	IR,R	1102,1110
ν_6	E_1'	IR	E_1	IR,R	1410,1410
ν_{10}	E_2'	R	E_2	R	1356,1351
ν_{13}	E_2'	R	E_2	R	897,885
ν_{14}	E_2''	--	E_2	R	597,569

The symmetric in plane CC stretch, ν_2, is expected to be the most intense feature in the Raman spectrum and to be strongly polarized (38). Accordingly, the very intense polarized Raman feature at 1126, 1124, 1124 cm^{-1} is the logical choice. Both of the antisymmetric ring stretches, ν_6 and ν_{10}, are expected to occur above 1300 cm^{-1}, a region relatively free of other absorptions in C_5H_5BeCl. On the basis of the IR - Raman activities, ν_6 and ν_{10} are easily assigned as

the features at 1427, 1435, 1430 cm^{-1} and 1352, 1352, 1352 cm^{-1}, respectively.

Of the two remaining ring vibrations the Raman only active in plane ring bend, ν_{13}, was observed in $(C_5H_5)_2Fe$ (37) at a higher frequency (897 cm^{-1} - in phase, 885 cm^{-1} - out of phase) than the corresponding out of plane ring bend, ν_{14}, (597 cm^{-1} - in phase, 569 cm^{-1} - out of phase). Moreover, by virtue of its inactivity under local D_{5h} symmetry, ν_{14} would be expected to have lower Raman intensity than ν_{13}. Accordingly, ν_{13} has been assigned as the moderately intense Raman band at 848, 843, 846 cm^{-1} and ν_{14} as the weaker Raman active only feature at 625, 622, 620 cm^{-1}. The weak infrared bands at 846 cm^{-1} and 838 cm^{-1} and the weak Raman shoulder at 842 cm^{-1} in solid C_5H_5BeCl are attributed to symmetry reduction and crystal splittings. The weak infrared feature in C_5H_5BeCl at 623 cm^{-1} may be the first overtone of the BeCl stretch ($2\nu_5' = 628$ cm^{-1}). Overlap with this overtone would also account for the low depolarization ratio (0.54) observed for the 624 cm^{-1} band in liquid C_5H_5BeCl.

In the above discussion all of the C_5H_5 vibrations were assigned in a manner consistent with the characteristic frequencies expected of such vibrations. Support was also obtained for the contention that very little coupling occurs between the vibrations of the ring and the metal tetrahydroborate group and therefore it is valid to discuss the vibrations in terms of local symmetries. When

comparing the frequencies of the assigned ring vibrations to the frequencies for $(C_5H_5)_2Fe$ (37) and $C_5H_5^-K^+$ (38) (see Table 16), the larger differences observed with respect to $C_5H_5^-K^+$ are further evidence that the compounds under investigation can be viewed as covalently bonded.

Vibrations of the Metal Tetrahydroborate Group

Local Symmetry and Number of Bridging Hydrogens

The number and activities of the fundamentals expected in boron - hydrogen terminal and bridge stretching and beryllium - hydrogen stretching regions will depend on whether the beryllium is singly, doubly, or triply hydrogen bridge bonded to the boron. Examination of the spectra in these regions thus determines the number of bridging hydrogens and consequently fixes the local symmetry of the metal tetrahydroborate group. The number and symmetries of the fundamentals expected in these regions for the possible bridging geometries are listed in Table 19.

Inspection of the boron - hydrogen terminal stretching region in both $C_5H_5BeBH_4$ and $C_5H_5BeBD_4$ clearly shows two strong bands, one of which is polarized. For a triply hydrogen bridged structure only one feature would be expected and therefore this structural possibility is ruled out. No evidence, however, can be obtained from this region which would distinguish between the single or double hydrogen bridge structures.

In the boron hydrogen bridge stretching region (1900-2200 cm^{-1}), one or two bands would be expected for a single or double bridge structure, respectively. For $C_5H_5BeBH_4$, only one strong, broad feature is observed, at ~2168 cm^{-1}, but for $C_5H_5BeBD_4$, two in-

Table 19. Number and symmetry[a] of the hydrogen stretching fundamentals for the possible bridging hydrogen geometries.

hydrogen stretching mode	single hydrogen bridge		double hydrogen bridge		triple hydrogen bridge	
	C_{3v}	C_s	C_{2v}	C_s[b]	C_{3v}	C_s
BH_t	A_1 E	2A' A''	A_1 B_1	A' A''	A_1	A'
BH_b	A_1	A'	A_1 B_2	2A'	A_1 E	2A' A''
BeH_b	A_1	A'	A_1 B_2	2A'	A_1 E	2A' A''

[a] All the vibrations of these symmetries are both infrared and Raman active.

[b] The C_s symmetry plane is assumed to be coincident with the plane of the bridging hydrogens (evidence for this will be presented later).

tense boron - deuterium stretches are clearly resolved at 1627 and 1574 cm^{-1}. Similar behavior has been observed for $BeBH_4^+$ in solid $Be(BH_4)_2$, a case where x-ray results have confirmed the presence of a double bridge.

Thus the terminal and bridge stretching regions alone suffice to establish a double bridge structure. Further support for this configuration will be presented in the following discussion of the vibrational assignments which will be based on a model of local C_{2v} symmetry. The vibrational frequencies cited in the discussion will be taken from Table 17 and will refer to $C_5H_5BeBH_4$. The corresponding $C_5H_5BeBD_4$ frequencies will be given in parentheses.

Terminal BH Stretches

Making the reasonable assumption that free rotation of the $BeBH_4$ group about the molecular symmetry axis does not occur, there are two likely orientations of the metal tetrahydroborate group relative to the C_s symmetry plane. If the $BeH_{2b}B$ bridging hydrogen plane were coincident with the C_s symmetry plane, one of the BH terminal stretches would be expected to be polarized and one would not. On the other hand if the BH_{2t} terminal hydrogen plane is coincident with the C_s symmetry plane, both BH terminal stretches would be expected to be polarized. That one polarized and one depolarized BH terminal hydrogen stretch is observed indicates that the $BeH_{2b}B$ bridg-

ing hydrogen and the C_s symmetry planes are coincident. The polarized behavior of other metal tetrahydroborate vibrations will also be examined with this point in mind.

While both of the terminal BH stretches are expected to be infrared and Raman active, only the symmetric BH stretch, ν_1', is expected to be polarized. Thus, of the two bands observed in the terminal BH stretching region, the strong polarized band at 2424 (1789) cm^{-1} is assigned as ν_1'. The remaining strong depolarized feature at 2475 (1864) cm^{-1} is assigned as the antisymmetric terminal BH stretch, ν_7'. As can be seen in Table 17, these values are in accord with the frequencies and splittings observed for the terminal BH stretches in $BeBH_4^+$ and $BeBD_4^+$ (15). The assignment of the antisymmetric terminal BH stretch at a higher frequency than the symmetric stretch is also consistent with the assignments reported for other cyclopentadienyl metal tetrahydroborates [$(C_5H_5)_2Zr(BH_4)_2$ (asym = 2440 cm^{-1}, sym = 2386 cm^{-1}), $(C_5H_5)_2Hf(BH_4)_2$ (asym = 2438 cm^{-1}, sym = 2380 cm^{-1})] (41). Assignment of the weak feature at 2447 (1834) cm^{-1} in the spectrum of $C_5H_5BeBD_4$ as the uncoupled BH(BD) terminal stretch of $C_5H_5BeBD_3H$, very near the average of the symmetric and antisymmetric BH terminal stretching frequencies at 2449 (1827) cm^{-1}, is further evidence for the correctness of the assignments of ν_1' and ν_7' and for the double bridge model.

Bridge BH Stretches

On the basis of Raman polarization data for liquid $C_5H_5BeBH_4$, the strong polarized Raman feature at 2166 cm^{-1} must be assigned as the symmetric bridge BH stretch, ν_2'. However, for the corresponding antisymmetric bridge BH stretch, ν_{10}', no other candidate is obvious. Thus, the strong infrared band at 2170 cm^{-1}, which could conceivably be construed as the infrared active counterpart of ν_2', is designated as ν_{10}' in $C_5H_5BeBH_4$. This choice gives an average value of 2168 cm^{-1} for the uncoupled bridge BH stretch, in good agreement with the 2167 cm^{-1} value observed for $C_5H_5BeBD_3H$.

For $C_5H_5BeBD_4$ the prominent bands at 1574 cm^{-1} and 1627 cm^{-1} are both polarized, as would be expected under C_s symmetry if the BeD_2B bridging hydrogen and C_s symmetry planes are coincident. On the basis of its greater Raman intensity and smaller depolarization value, the 1574 cm^{-1} band in $C_5H_5BeBD_4$ is assigned as the symmetric bridge BD stretch, ν_2'. The corresponding antisymmetric bridge BD stretch, ν_{10}', is then assigned at 1627 cm^{-1}. As can be seen from Table 17 these assignments give a frequency ordering and H/D ratios which are in good agreement with the values for $BeBH_4^+$ (15).

Bridge BeH Stretches

Just as for the bridge BH stretching region, only one strong, rather broad feature is observed in the bridge BeH stretching region

of $C_5H_5BeBH_4$. Because of its breadth, and the presence of two maxima at 1477 cm^{-1} and 1471 cm^{-1}, this feature is thought to contain both ν'_{11} and ν'_3. Though the choice of either one of these frequencies as the symmetric or antisymmetric BeH bridge stretch is somewhat arbitrary, the higher value, 1477 cm^{-1}, is assigned as the symmetric ν'_3 bridge BeH stretch by analogy with solid $BeBH_4^+$ (15). Similarly, for $C_5H_5BeBD_4$ one strong band exhibiting two maxima, at 1092 cm^{-1} and 1086 cm^{-1}, is observed in the infrared. The proximity of strong C_5H_5 ring bands obscured the polarization data for these bands. Thus, principally on the basis of its Raman intensity, the band at 1086 cm^{-1} is chosen as ν'_3, the symmetric bridge BeH stretch and therefore the 1092 cm^{-1} band must be chosen as ν'_{11}, the antisymmetric bridge BeH stretch. Of the other bands in the bridge BeH and BeD stretching regions the close frequency correspondence in going from $C_5H_5BeBD_4$ to $C_5H_5BeBH_4$to C_5H_5BeCl favored their assignment as vibrations of the C_5H_5 ring. The near coincidences of the symmetric and antisymmetric bridge BH, BeH, BeD stretches are somewhat surprising in view of their bonding to common atoms (the analogous symmetric - antisymmetric splittings in the similar systems $BeBH_4^+$ and $BeBD_4^+$ (15) average 69 cm^{-1}).

Bending Vibrations

Five bending vibrations are expected in the region 200 - 1300

cm^{-1}. Of these modes all but ν_9', the $BeH_{2b}B$ bridge bend, lie above 600 cm^{-1}. The bridge bend has previously been assigned at 405 (346) cm^{-1} for $BeBH_4^+$ and at 255 (194) cm^{-1} for $Al(BH_4)_3$. In this region for $C_5H_5BeBH_4$, the medium Raman feature at 328 (271) cm^{-1} appears to be the best choice for ν_9' since the H/D ratio of only this pair of bands (1.21) is high enough to be comparable to the ratios observed for $BeBH_4^+$ (1.17) and $Al(BH_4)_3$ (1.31). This frequency value, halfway between those of $BeBH_4^+$ and $Al(BH_4)_3$, does not, as will be shown later, reflect the relative strength of the bridge bonding in these compounds. It is also worth noting that, although strongly overlapped with neighboring bands, this mode seems to be depolarized - a result in accord with the suspected coincidence of the $BeH_{2b}B$ and C_s planes.

The four remaining bending motions can be thought of as a deformation, a torsion, a rock,and a wag of the terminal BH_{2t} group. All of these modes are both infrared and Raman active under C_{2v} symmetry, except the torsion which is Raman active only. The occurence of a strong, sharp, and, in general, polarized band between 1100 cm^{-1} and 1150 cm^{-1} is characteristic of the BH_{2t} deformation of molecules containing doubly bridged tetrahydroborate groups. This band has been assigned in $Al(BH_4)_3$ at 1113 (850) cm^{-1}, in $BeBH_4^+$ (15) at 1128 (823) cm^{-1}, in $(C_5H_5)_2TiBH_4$ (42) at 1123 cm^{-1}, and in $(C_5H_5)_2Zr(BH_4)_2$ (41) at 1123 cm^{-1}. Accordingly, the strong infrared feature at 1131 cm^{-1} in $C_5H_5BeBH_4$ is chosen as ν_4', the BH_{2t} deformation. Several possibilities (938, 862, 847 cm^{-1}) exist in the spectra of $C_5H_5BeBD_4$ for

the assignment of the BD_t deformation, ν_4'. Of these the strong infrared, weak Raman feature at 938 cm^{-1} gives an H/D ratio of 1.21, which is lower than expected [$Al(BH_4)_3$ H/D = 1.31, CH_3BeBH_4 H/D = 1.30 (43), $BeBH_4^+$ H/D = 1.37 (15), and B_2H_6 H/D = 1.29 and 1.35 (44)]. It does, however, parallel the intensity behavior of the 1131 cm^{-1} $C_5H_5BeBH_4$ band and on this basis is assigned as ν_4'. Assignment of the weak infrared, moderate Raman feature at 847 cm^{-1} would give a better H/D ratio (1.34), but the wrong intensity pattern. More importantly, the 847 cm^{-1} band is the only logical choice as ν_5' in $C_5H_5BeBD_4$. Finally, the only other possibility, the strong infrared, weak Raman feature at 862 cm^{-1} is for more compelling reasons assigned as a ring vibration. The low H/D ratio for ν_4' is perhaps reasonable since this mode can be expected to mix significantly with the $C_5H_5BeBD_4$ skeletal stretch, ν_5', at 847 cm^{-1} (H/D = 1.05).

The Raman active torsional mode ν_6' is assigned as the medium Raman feature at 1173 cm^{-1} on the basis of its absence in the infrared spectrum and by analogy with an $Al(BH_4)_3$ value of 1155 (813) cm^{-1}. The corresponding twist for $C_5H_5BeBD_4$ would be expected to fall at a frequency lower by the $\sqrt{2}$ since only hydrogen motion is involved in this mode. Thus it is believed that ν_6' for $C_5H_5BeBD_4$ is buried in the overlapping structure near 836 cm^{-1} (H/D = 1.40). This mode was not assigned previously for $BeBH_4^+$ since BH_4^- features obscure the 1170 (830) cm^{-1} region, but there do not seem to be any inconsistencies with the present choice. A slightly higher value than for $Al(BH_4)_3$ is consistent with a slightly stronger bridge bond (as had

been deduced from the bridge bending region).

The assignments of the remaining bending vibrations, the BH_{2t} rock and wag, are rather arbitrary and owe as much to the previous elimination of other possibilities as to any argument advanced in their behalf. Consistent with the assignment of the BH_{2t} rock in $Al(BH_4)_3$ at 967 (735) cm^{-1} and in CH_3BeBH_4 (43) at 898 (667) cm^{-1}, the moderate (weak) band at 990 (750) cm^{-1} is assigned as ν'_8. The measured H/D ratio of 1.32 for this band is in close agreement with the H/D ratios observed for $Al(BH_4)_3$ and CH_3BeBH_4 (43) of 1.32 and 1.35, respectively. Few choices remain for the assignment of the BH_{2t} wag. In view of the assignment of this mode in $Al(BH_4)_3$ at 779 cm^{-1} (in phase) and 723 cm^{-1} (out of phase), the strong infrared, weak Raman band at 823 (704) cm^{-1} is assigned as the BH_{2t} wag, ν'_{12}. It is worth noting that in $C_5H_5BeBD_4$, ν'_{12} at 704 cm^{-1} is polarized as would be expected under C_s symmetry for coincident $BeD_{2b}B$ bridging and C_s symmetry planes. The only metal tetrahydroborate vibration not yet assigned, the BeB stretch, will be discussed in the following section on skeletal vibrations, where it is more logically juxtaposed with the discussion of the assignment of the C_5H_5Be stretch.

Skeletal Vibrations

When the C_5H_5 and $BeBH_4$ units combine to form the $C_5H_5BeBH_4$ molecule, three rotational and three translational degrees of free-

dom are converted to six vibrational modes: ν_1'', a C_5H_5...Be stretch; ν_2'', ν_3'', a ring tilt; ν_4'', ν_5'', a C_5H_5BeX ring - metal - ligand bend; and ν_6'', a torsion. The tilting and bending modes are both doubly degenerate under C_{5v} symmetry and can be expected to split under C_s symmetry, each yielding one polarized and one depolarized vibration. The torsion is expected to be the lowest lying of the skeletal modes. On the basis of this, and the observation of the torsion in $(C_5H_5)_2Ru$ (37) at 130 cm^{-1}, the moderate $C_5H_5BeBH_4$ Raman band at 182 (152) cm^{-1} is assigned as the torsion, ν_6''. This higher value compared to $(C_5H_5)_2Ru$ is reasonable in view of the lower inertial moment of the BH_4 group. The relatively low H/D ratio of 1.20 observed for the torsion is probably due to mixing of this mode with the nearby C_5H_5BeX ring - metal - ligand bend.

In both $(C_5H_5)_2Fe$ and $(C_5H_5)_2Ru$ (37), the ring - metal - ligand bend (179 cm^{-1} and 170 cm^{-1}, respectively) is sensibly assigned at a lower frequency than the ring tilts (389, 492 cm^{-1} and 400, 450 cm^{-1}, respectively). Accordingly, the strong depolarized Raman feature at 176, 220, 214 cm^{-1} is chosen as the C_5H_5BeX ring - metal - ligand bend. No splitting was resolved for these bands in $C_5H_5BeH_4$ and $C_5H_5BeBD_4$, hence ν_4'' and ν_5'' are assumed degenerate. The observed H/D ratio of 1.03 is slightly higher than the calculated value of 1.01, reflecting some mix with the torsional mode.

The other "degenerate" mode, the ring tilt, is assigned as the strong depolarized Raman feature at 482 cm^{-1} in C_5H_5BeCl. In

both $C_5H_5BeBH_4$ and $C_5H_5BeBD_4$ the ring tilt is observed to be split slightly. Rather arbitrarily, the ring tilt in the C_s symmetry plane is assigned to the lower frequency component. Thus, ν''_3 = 497 (509) and ν''_4 = 488 (497) cm^{-1}. These values are noticeably higher than for $(C_5H_5)_2Fe$, an observation consistent with the shorter metal - ring bond found for Be (1.48Å) compared to Fe (1.60Å).

There remains the C_5H_5...Be and Be...BH_4 stretching modes to be discussed. Both of these modes should be polarized and, indeed, two strong polarized Raman features stand out for each of C_5H_5BeCl (920, 314 cm^{-1}) $C_5H_5BeBH_4$ (888, 392 cm^{-1}), and $C_5H_5BeBD_4$ (847, 366 cm^{-1}). There is, however, some uncertainty as to which of these frequencies should be described as the C_5H_5Be stretch and which as the $BeBH_4$ stretch. For $(C_5H_5)_2Be$, a compound in which the Be atom is 1.48 Å from one ring but 1.98 Å from the other, we have measured the stretches at 597 and 316 cm^{-1}. In this instance, the higher stretch would logically be associated with the shorter bond. Since this shorter bond remains essentially unchanged when the second C_5H_5 group is replaced by Cl, BH_4, or BD_4 (Table 20), it might be expected that this stretching mode would remain near 600 cm^{-1}. Clearly this is not the case for C_5H_5BeCl, $C_5H_5BeBH_4$, or $C_5H_5BeBD_4$, and hence this raises the question of whether C_5H_5Be stretch shifts up or down in the latter compounds. To examine this point further, several simple calculations were made.

Table 20. Bond distance (Å), skeletal frequencies (cm^{-1}), eigenvectors and force constants[a] for xyz models of relevant molecules.

x	y	z	r_{xy}	r_{yz}	ν_{obs}	ν_{calc}	Eigenvectors Δr_{xy}	Eigenvectors Δr_{yz}	k_{xy}	k_{yz}	k_{xz}	k_{α}
C_5H_5	Be	BH_4	1.484	1.88	888	887	0.60	-1.00				
					392	389	1.00	-0.07				
					220	218	---	---				
									1.576	3.419	1.143	0.150
C_5H_5	Be	BD_4	1.484	1.88	847	848	0.67	-1.00				
					366	369	1.00	-0.03				
					214	216	---	---				
C_5H_5	Be	C_5H_5	1.98	1.48	597	600	-0.24	-1.00				
					316	276	1.00	0.14	(1.576)[b]	2.606	1.223	0.128
					190	190	---	---				
C_5H_5	Be	Cl	1.484	1.837	920	920	0.83	-1.00				
					314	314	1.00	0.14	(1.576)[b]	3.905	0.845	0.101
					176	176	---	---				
Cl	Be	Cl	1.75	1.75	1113	1113	1.00	-1.00				
					---	488	1.00	1.00	(3.905)[c]	(3.905)[c]	0.993	0.836
					482	482	---	---				
BH_4^-	^+Be	BH_4	2.02	1.92	725	725	0.62	-1.00				
					640	640	1.00	-0.01				
					202	199	---	---				
									2.234	2.621	1.399	0.157
BD_4^-	^+Be	BH_4	2.02	1.92	700	700	0.79	-1.00				
					575	575	1.00	0.24				
					192	194	---	---				

Table 20. Bond distance (Å), skeletal frequencies (cm^{-1}), eigenvectors and force constants[a] for xyz models of relevant molecules.

---

[a] Force constant units are millidyne/Å, except k_α, which is in ergs/ rad^2 x 10^{-11}.

[b] Fixed at the $C_5H_5BeBH_4$ value since problem is undetermined.

[c] Fixed at the C_5H_5BeCl value since problem is undetermined.

First, one might hope that the H → D isotope effect on these stretching frequencies would be revealing. Of course, a detailed calculation using the entire molecule is not practical, but a calculation based on a simple diatomic point mass model is easily performed. One can distinguish three limiting cases here, $(C_5H_5)\ldots(BeBH_4)$, $(C_5H_5Be)\ldots(BH_4)$, or $Be\ldots(BH_4)$. The calculated H/D ratios for these three extremes are 1.06, 1.10, and 1.04, respectively. The observed H/D ratios are 888/847 = 1.05, 392/366 = 1.07. Unfortunately, these results could be taken to favor either assignment since it is not known which of the two descriptions, $(C_5H_5Be)\ldots(BH_4)$ or $Be\ldots(BH_4)$, best describes the Be...B stretch.

In an effort to improve this calculation, further computations (Table 20) based on a linear x - y - z point mass model were made. A non-linear least squares force constant refinement program (45) was used for these calculations. For C_5H_5BeCl and $(C_5H_5)_2Be$, not enough data was available to explicitly determine all the force constants, and therefore for these systems $k_{C_5H_5\ldots Be}$ was assumed to be equal to the value found for $C_5H_5BeBH_4$. Even with this constraint, the $(C_5H_5)_2Be$ problem was reluctant to converge because of a strong correlation between k_{yz} and k_{xz}.

A number of points can be made about the results presented in Table 20. First, the eigenvectors for $C_5H_5BeBH_4$ and C_5H_5BeCl clearly

show that the lowest stretching frequency (314, 392, 366 cm^{-1}) is predominantly the C_5H_5...Be stretch, ν_1''. The higher frequency (920, 888, 847 cm^{-1}) in turn involves an excess of Be...BH_4 or BeCl stretching (ν_5'), although there is sufficient mixing of coordinates that a reasonable alternative description might be to talk of an antisymmetric movement of the Be atom against the two ligands. Certainly the stretch - stretch interaction force constant is large for all the molecules listed and hence some coupling of the coordinates is expected.

A second point worth noting is the unusual result for $(C_5H_5)_2Be$. Here, because of the equal C_5H_5 masses, no a priori association of a bond length with a force constant can be made. Because the problem for $(C_5H_5)_2Be$ is undetermined, the C_5H_5Be force constant associated with the shorter C_5H_5Be bond distance (1.48 Å) was assumed from the value determined for $C_5H_5BeBH_4$. Thus the other C_5H_5Be force constant in $(C_5H_5)_2Be$ was expected to be lower in value, reflecting the larger C_5H_5Be bond (1.98 Å). In fact, convergence was only achieved (with difficulty) with a <u>larger</u> value for the second C_5H_5 force constant. The only sensible interpretation of this result seems to be that, although the shorter C_5H_5Be distance (1.48 Å) is unchanged in going from $C_5H_5BeBH_4$ to $(C_5H_5)_2Be$, the corresponding force constant does increase significantly to 2.606 millidynes/Å from 1.576 millidynes/Å. Thus, in Table 20, the labeling of the bond lengths is chosen to reflect this fact.

Finally, it may be observed that the $BeBH_4$ stretching force

constant is noticeably stronger for $C_5H_5BeBH_4$ than for $^+BeBH_4$, a result which is consistent with stronger bridge and shorter Be...B distance in the former compound.

Lattice and Combination Bands

A number of other features were observed in the spectra of C_5H_5BeCl, $C_5H_5BeBH_4$, and $C_5H_5BeBD_4$, and most are satisfactorily assigned as combination bands, overtones, or as crystal splitting of fundamentals as indicated in Tables 13, 14, and 15. The choices for the overtone and combination bands were made on the basis of activities, frequency fit, intensities of the parent fundamentals, and the probability of significant coupling. In no instances were other than binary combinations resorted to in assigning the bands. That all of the observed features were reasonably assigned is taken as support for the fundamental assignments.

In addition, several lattice vibrations were observed in the Raman spectra of the solid phase. However, since the crystal structures of the compounds are unknown, no arguments can be advanced concerning the expected activities of such modes.

Product Rule Calculations

Table 21 lists the moments of inertia calculated from the structural parameters determined by Drew (36) for doubly hydrogen bridged $C_5H_5BeBH_4$ and $C_5H_5BeBD_4$. The theoretical product rule factors and the observed results for both the molecule as a whole (C_s symmetry) and the metal tetrahydroborate group (C_{2v} symmetry) are also shown in Table 21. Considering that anharmonicity usually gives an observed factor which is less than the theoretical result, the agreement based on the C_{2v} model is fair and the product rule calculations can be said to support the assignments. The poorer results obtained for the C_s symmetry model in part reflect the inclusion of the skeletal torsion, ν_6'', whose H/D ratio of 1.20 is lower than expected.

Structural Inferences from the Spectra

Consideration of the activities in the terminal and bridge hydrogen stretching regions clearly favors the double hydrogen bridge model (C_{2v} symmetry) over the single or triple hydrogen bridge models (C_{3v} symmetries) for $C_5H_5BeBH_4$ and $C_5H_5BeBD_4$. Moreover, the observation that the frequencies of the uncoupled BH(BD) stretches in $C_5H_5BeBD_3H$ are very close to the average values of the symmetric and antisymmetric stretches implies that two equivalent BH bonds are con-

Table 21. Product rule calculations for $C_5H_5BeBH_4$ and $C_5H_5BeBD_4$.

Moments of inertia	$C_5H_5BeBH_4$	$C_5H_5BeBD_4$
Cs (entire molecule)		
I_x (Amu-Å^2)	204.39	235.53
I_y (Amu-Å^2)	203.68	234.20
I_z (Amu-Å^2)	119.99	124.91
M (Amu)	88.89	92.92
C_{2v} ($BeBH_4$ unit only)		
I_x (Amu-Å^2)	23.82	29.54
I_y (Amu-Å^2)	23.20	28.30
I_z (Amu-Å^2)	4.92	9.84
M (Amu)	23.85	27.88
Product rule factor	**Calc.**	**Obs.**
C_s (entire molecule)		
A' $(D/H)^{7/2}[M(H)/M(D)][I_x(H)/I_x(D)]^{1/2}$	10.06	8.764
A'' $(D/H)^{5/2}[M(H)I_z(H)I_y(H)/M(D)I_z(D)I_y(D)]^{1/2}$	5.048	3.002

Table 21. Product rule calculations for $C_5H_5BeBH_4$ and $C_5H_5BeBD_4$. (Continued)

C_{2v} ($BeBH_4$ unit only)			
A_1	$(D/H)^2[M(H)/M(D)]^{1/2}$	3.694	3.219
A_2	$(D/H)[I_z(H)/I_z(D)]^{1/2}$	1.413	1.403
B_1	$(D/H)^{3/2}[M(H)I_y(H)/M(D)I_y(D)]^{1/2}$	2.366	2.124
B_2	$(D/H)^{3/2}[M(H)I_x(H)/M(D)I_x(D)]^{1/2}$	2.346	2.101

tained in the molecule. Since there is only one tetrahydroborate group per molecule, the presence of two equivalent BH bonds constitutes further evidence for the double bridge. Finally, comparison of the frequency values with those expected for single, double, and triple hydrogen bridge structures (see Table 6) shows the observed frequencies to be most in accord with the double hydrogen bridge structure.

Two orientations of the tetrahydroborate group with respect to the ring are possible. If the $BeH_{2b}B$ bridging hydrogen plane is coincident with the C_s symmetry plane, the B_1 metal tetrahydroborate vibrations $\nu'_{7...9}$ are expected to be depolarized, while the B_2 vibrations $\nu'_{10...12}$ should be polarized. If, however, the BH_{2t} terminal hydrogen plane is coincident with the C_s symmetry plane, the above polarization behavior would be reversed. Since, theoretically, the depolarization ratio of a polarized mode may equal that expected for a depolarized mode (ρ = 0.75 for linearly polarized incident radiation), the observation of polarized behavior (as opposed to depolarized behavior) must be taken as the more compelling evidence for a particular orientation. Of the above bands ν'_{10} and ν'_{12} in $C_5H_5BeBD_4$ are found to be polarized. Furthermore, ν'_{10} is not observed in the perpendicular polarization of the Raman spectrum of liquid $C_5H_5BeBH_4$ where, if depolarized, it might be expected to appear, since in this polarization the intensity of the overlapping strongly polarized ν'_2 would be greatly reduced. These results can be viewed as strong evi-

dence for the coincidence of the C_s and $BeH_{2b}B$ hydrogen planes.

In addition to the observation that C_5H_5BeCl, $C_5H_5BeBH_4$, and $C_5H_5BeBD_4$ are volatile compounds with low melting points, the similarities observed in the spectra of the liquid and solid phases suggest that these compounds are covalently bonded in these phases. Other similarities between the frequencies of the assigned C_5H_5 ring fundamentals in C_5H_5BeCl, $C_5H_5BeBH_4$, $C_5H_5BeBD_4$ further suggest that there is very little coupling between the ring vibrations and the rest of the molecule and thus justify the assignment of the ring and metal tetrahydroborate fundamentals on the basis of C_{5v} and C_{2v} local symmetries, respectively.

Summary

In this work, the vibrational fundamentals in C_5H_5BeCl, $C_5H_5BeBH_4$, and $C_5H_5BeBD_4$ are assigned and, for the latter two compounds, are found to be in agreement with the product rule. For $C_5H_5BeBH_4$ and $C_5H_5BeBD_4$ the spectra are satisfactorily interpreted in terms of a covalent double hydrogen bridge structure in which the plane of the bridging hydrogens is found to be coincident with the C_s symmetry plane. The observed similarities for the C_5H_5 ring fundamentals in all three compounds suggest negligible coupling between the ring and metal tetrahydroborate groups and thus support the assignment of the group vibrations in terms of local C_{5v} and C_{2v} symmetries, respectively.

BIBLIOGRAPHY

1. A. Stock, "Hydrides of Boron and Silicon" (Cornell University Press, Ithaca, New York, 1933).

2. H. I. Schlesinger, R. T. Sanderson, and A. B. Burg, J. Am. Chem. Soc. 62, 3421 (1940).

3. A. B. Burg and H. I. Schlesinger, J. Am. Chem. Soc. 62, 3425 (1940).

4. H. I. Schlesinger and H. C. Brown, J. Am. Chem. Soc. 62, 3429 (1940).

5. B. D. James and M. G. H. Wallbridge in: "Progress in Inorganic Chemistry", edited by S. J. Lippard (Wiley-Interscience, New York, 1970), Vol. 11, p. 99.

6. Y. Matsui and R. C. Taylor, J. Am. Chem. Soc. 90, 1363 (1968).

7. H. C. Brown and P. A. Tierney, J. Am. Chem. Soc. 80, 1552 (1958).

8. J. W. Nibler, J. Am. Chem. Soc. 94, 3349 (1972).

9. G. Gunderson, L. Hedberg, and K. Hedberg, J. Chem. Phys. 59, 3777 (1973).

10. E.R. Bernstein, W. C. Hamilton, T. A. Keiderling, S. J. LaPlaca, S. J. Lippard, and J. J. Mayerle, Inorganic Chemistry 11, 3009 (1972).

11. P. H. Bird and M. R. Churchill, Chem. Comm., 403 (1967).

12. V. Plato and K. Hedberg, Inorganic Chemistry 10, 590 (1971).

13. N. Davies, M. G. H. Wallbridge, B. E. Smith, and B. D. James, J. Chem. Soc.- Dalton Trans., 162 (1973).

14. T. J. Marks and L. A. Shimp, J. Am. Chem. Soc. 94, 1542 (1972).

15. J. W. Nibler, D. F. Shriver, and T. H. Cook, J. Chem. Phys. 54, 5257 (1971).

16. D. S. Marynick and W. N. Lipscomb, J. Am. Chem. Soc. 93, 2322 (1971).

17. J. W. Nibler and T. H. Cook, J. Chem. Phys. 58, 1596 (1973).

18. N. A. Bailey, P. H. Bird, N. Davies, and M. G. H. Wallbridge, J. Inorg. and Nuc. Chem. 32, 3116 (1970).

19. P. C. Maybury and J. C. Ahnell, Inorg. Chem. 6, 1286 (1967).

20. R. A. Ogg and J. D. Ray, Diss. Farad. Soc. 19, 215 (1955).

21. R. E. Williams, J. Inorg. and Nuc. Chem. 20, 198 (1961).

22. R. V. Ammon, B. Kannellakopulos, G. Schmid, and R. D. Fischer, J. Organometal. Chem. 25, C1 (1970).

23. C. H. Bushweller, H. Beall, M. Grace, W. J. Dewkett, and H. S. Bilofsky, J. Am. Chem. Soc. 93, 2145 (1971).

24. H. I. Schlesinger, H. C. Brown, and E. K. Hyde, J. Am. Chem. Soc. 75, 209 (1953).

25. D. A. Drew and G. L. Morgan (Dept. of Chem., University of Wyoming, Laramie, Wyoming), unpublished results.

26. T. H. Cook, present address: Dept. of Physical Sciences, Nebraska Western College (Scottsbluff, Nebraska).

27. Air Products and Chemicals, Inc., "Cryo-Tip Instruction and Operating Manual", Advanced Products Dept., Allentown, Penn. (Air Products and Chemicals, Inc., 1967).

28. Air Products and Chemicals, Inc., "Technical Manual for Displex TM 77°K Helium Refrigerator", Advanced Products Dept., Allentown, Penn. (Air Products and Chemicals, Inc., 1971).

29. Beckman Instruments Inc., "IR-7 Infrared Spectrophotometer Instruction Manual", (Beckman Instruments Inc., Fullerton, Calif., 1960).

30. The Perkin - Elmer Corp., "Operating Instructions Model 180 Infrared Spectrometer", (The Perkin - Elmer Corp., Norwalk, Conn., 1970).

31. J. W. Nibler, D. Coe, M. Lesiecki, H. Rojhantalab, and E. Suzuki, Raman Newsletter 59, 12 (1973).

32. A. Almenningen, G. Gunderson, and A. Haaland, Acta Chem. Scand. 22, 328 (1968).

33. W. C. Price, J. Chem. Phys. 17, 1044 (1949).

34. A. R. Emery and R. C. Taylor, Spectrochim. Acta 16, 1455 (1960).

35. D. A. Drew and A. Haaland, Acta Chem. Scand. 26, 3351 (1972).

36. D. A. Drew, G. Gunderson, and A. Haaland, Acta Chem. Scand. 26, 26 (1972).

37. J. S. Bodenheimer and W. Low, Spectrochim. Acta 29A, 1733 (1973).

38. H. P. Fritz in: "Advances in Organometallic Chemistry", edited by F. G. A. Stone and R. West (Academic Press, New York, 1964) Vol. 1, p. 240.

39. E. M. Suzuki and J. W. Nibler, Spectrochim. Acta 30A, 15 (1974).

40. R. C. Lord and D. G. Rea, J. Am. Chem. Soc. 79, 2401 (1957).

41. N. Davies, B. D. James, and M. G. H. Wallbridge, J. Chem. Soc. A, 2223 (1969).

42. V. H. Nöth, E. Wiberg, and L. P. Winter, Zeitschrift anorganische and allgemeine Chemie 370, 209 (1969).

43. T. H. Cook and G. L. Morgan, J. Am. Chem. Soc. 92, 6487 (1970).

44. W. J. Lehmann, J. F. Ditter, and I. Shapiro, J. Chem. Phys. 29, 1248 (1958).

45. J. H. Schachtschneider, "Vibrational Analysis of Polyatomic Molecules. VI", (Shell Development Company, Emeryville, California, 1964), Technical Report No. 57-65.